MIAMI

Microscopes and
Ion Accelerators for
Materials Investigations

University of Huddersfield

Experimental techniques for radiation damage effects: In-situ Ion-Irradiation in a Transmission Electron Microscope

S E Donnelly

School of Computing and Engineering

University of Huddersfield, UK

EPSRC

Engineering and Physical Sciences Research Council

Joint ICTP-IAEA Workshop on Radiation Effects in Nuclear Waste Forms
and their Consequences for Storage and Disposal,
Trieste, 12–16 September 2016

University of HUDDERSFIELD

Huddersfield

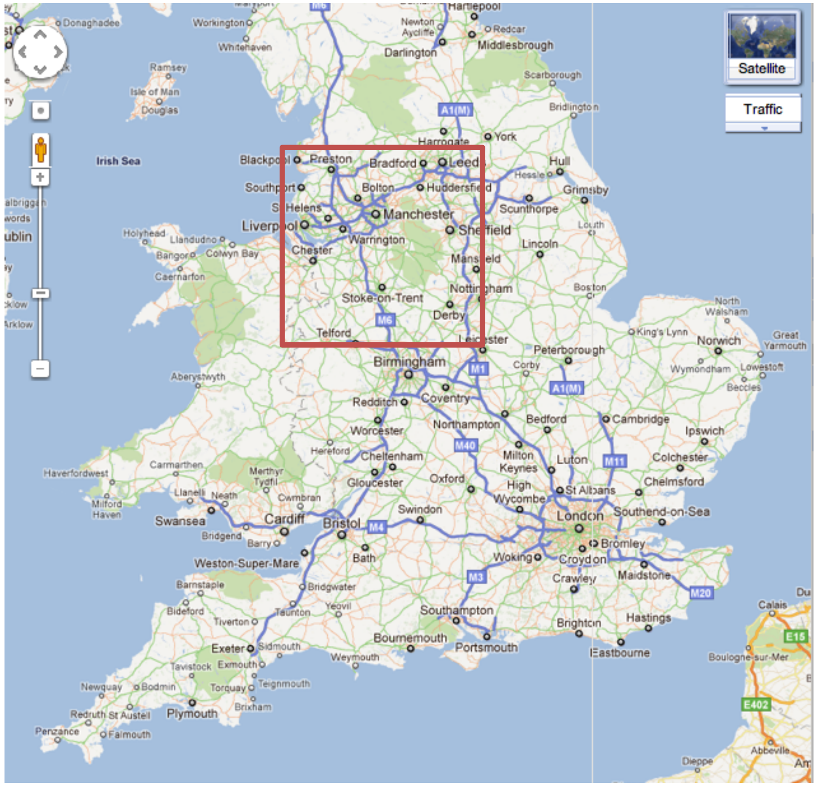

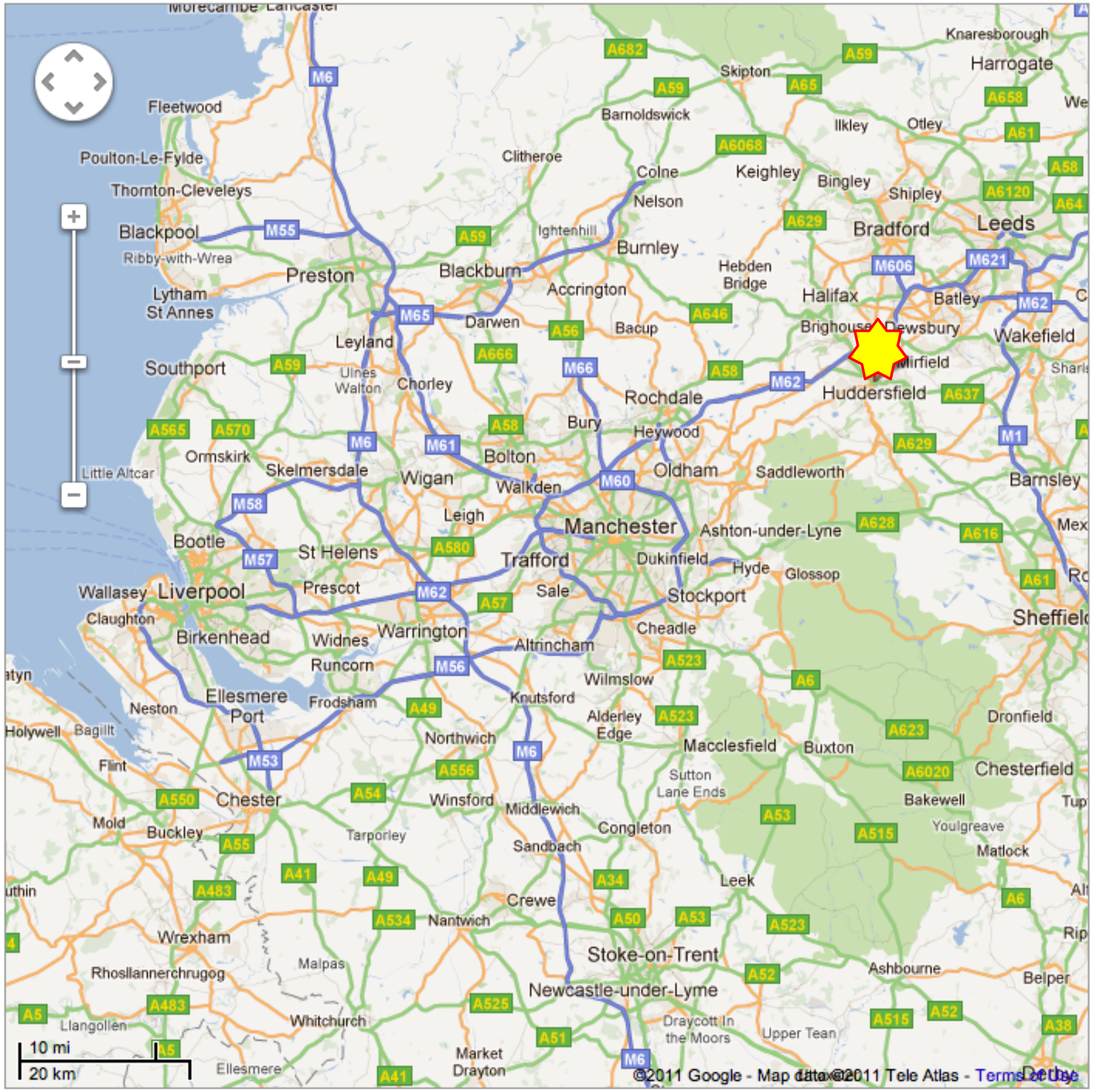

http://www.geograph.org.uk/photo/1887670

Google maps

In-Situ TEM[*] / Ion-Accelerator Facilities

[*]Transmission Electron Microscope

In-situ TEM / ion accelerator facilities

University of HUDDERSFIELD

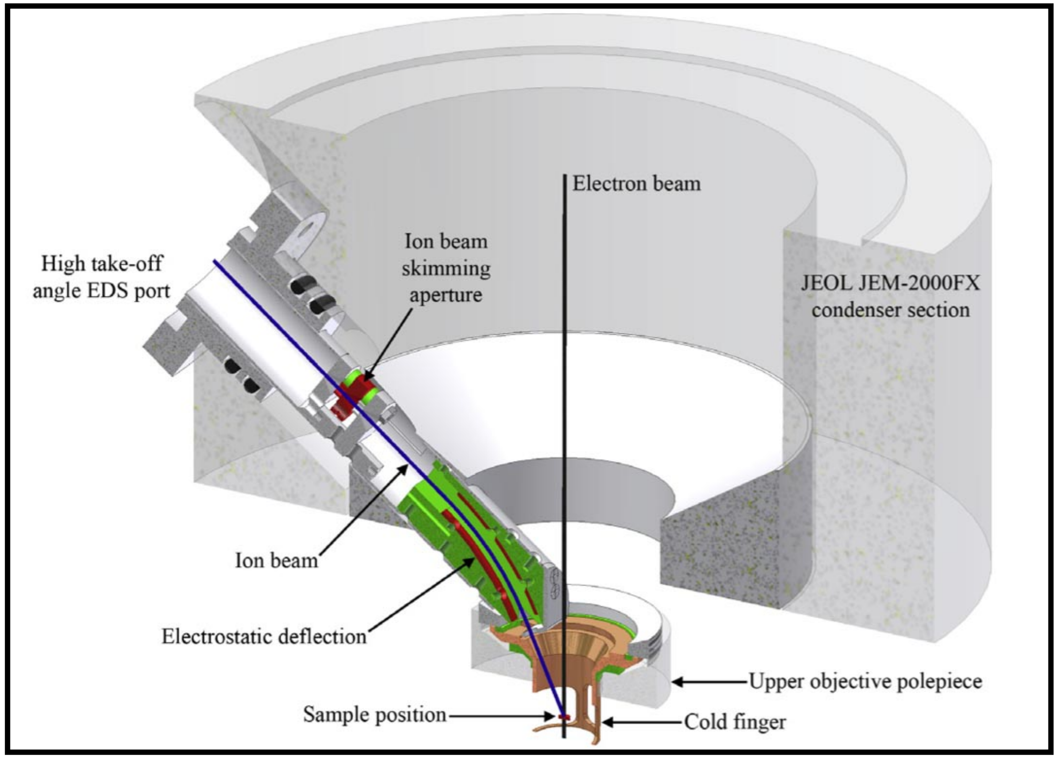

Experimental systems combining one or more ion-accelerators with a transmission electron microscope (TEM) enabling observation of ion-beam induced radiation damage at high magnification in real time.

Permit study of the formation and development of defects at the nanoscale during ion irradiation, often providing insights into fundamental properties and processes that are difficult to obtain by other means.

Also allows irradiation and observation to be carried out at low temperatures. This can be difficult to do with separate ion accelerators and microscopes.

In-situ TEM / ion accelerator facilities

University of HUDDERSFIELD

Kyushu, Japan

Argonne, USA

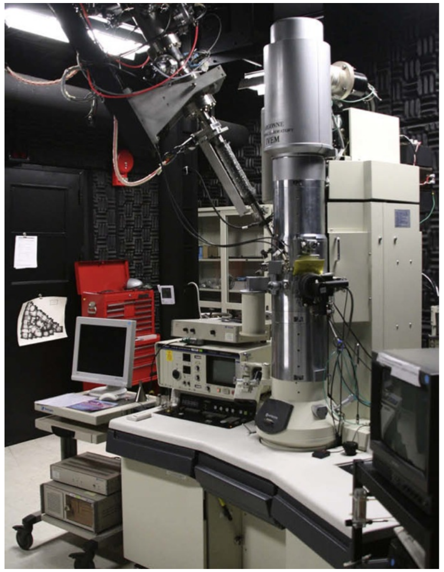

Hokkaido, Japan

Tsukuba, Japan

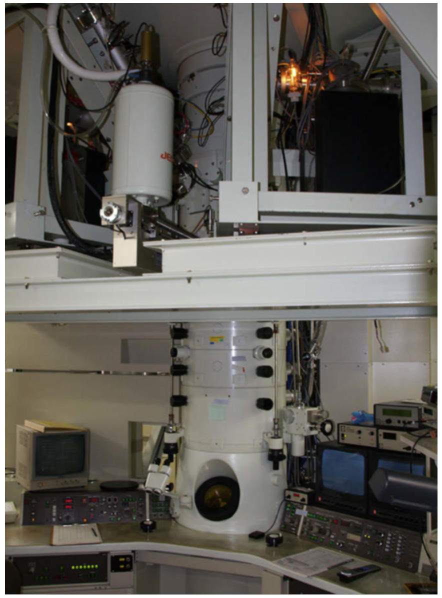

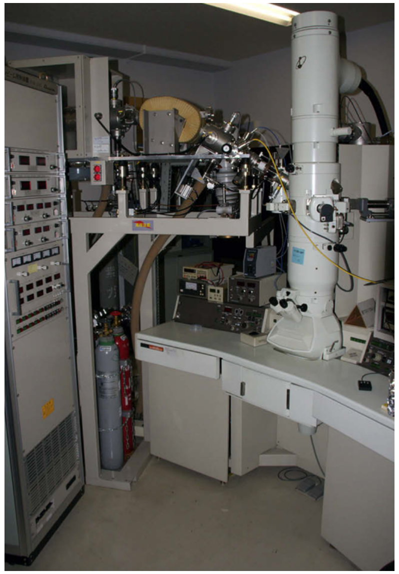

Shimane, Japan

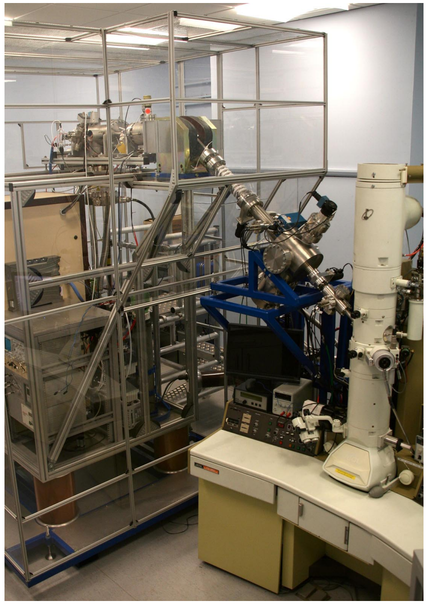

Huddersfield, UK

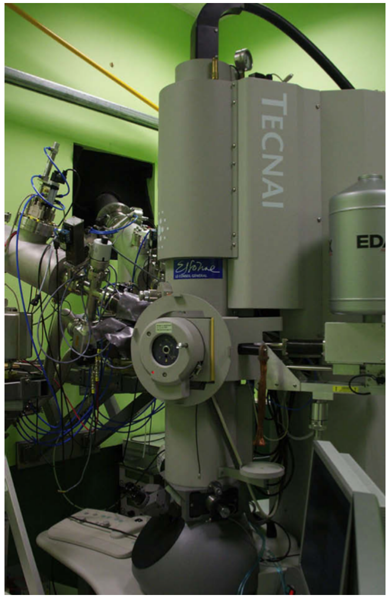

Orsay, France

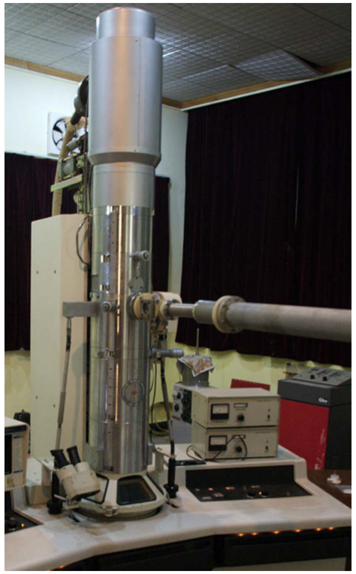

Wuhan, China

Sandia.USA

Applications

Investigations into any materials subjected to radiation damage from energetic particles, such as:

- Semiconductor processing and damage to microelectronic devices used in irradiating environments;
- Materials in space;
- Nanotechnology – e.g. use of ion beams to create or modify nanostructures;
- Materials for nuclear fission (current and Gen IV) and nuclear fusion. Glasses and ceramics for nuclear waste storage.

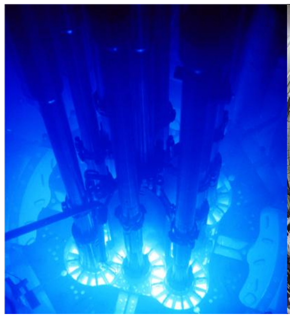
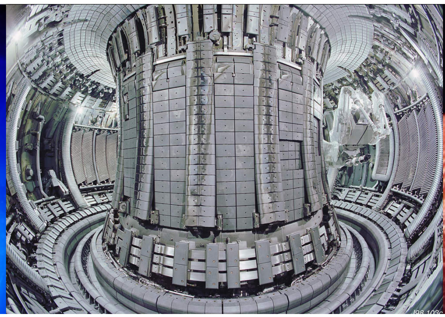


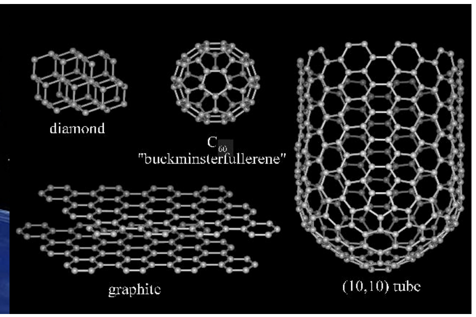

Interfacing an Ion-Beam System with a TEM

Transmission Electron Microscope (TEM)

University of Huddersfield

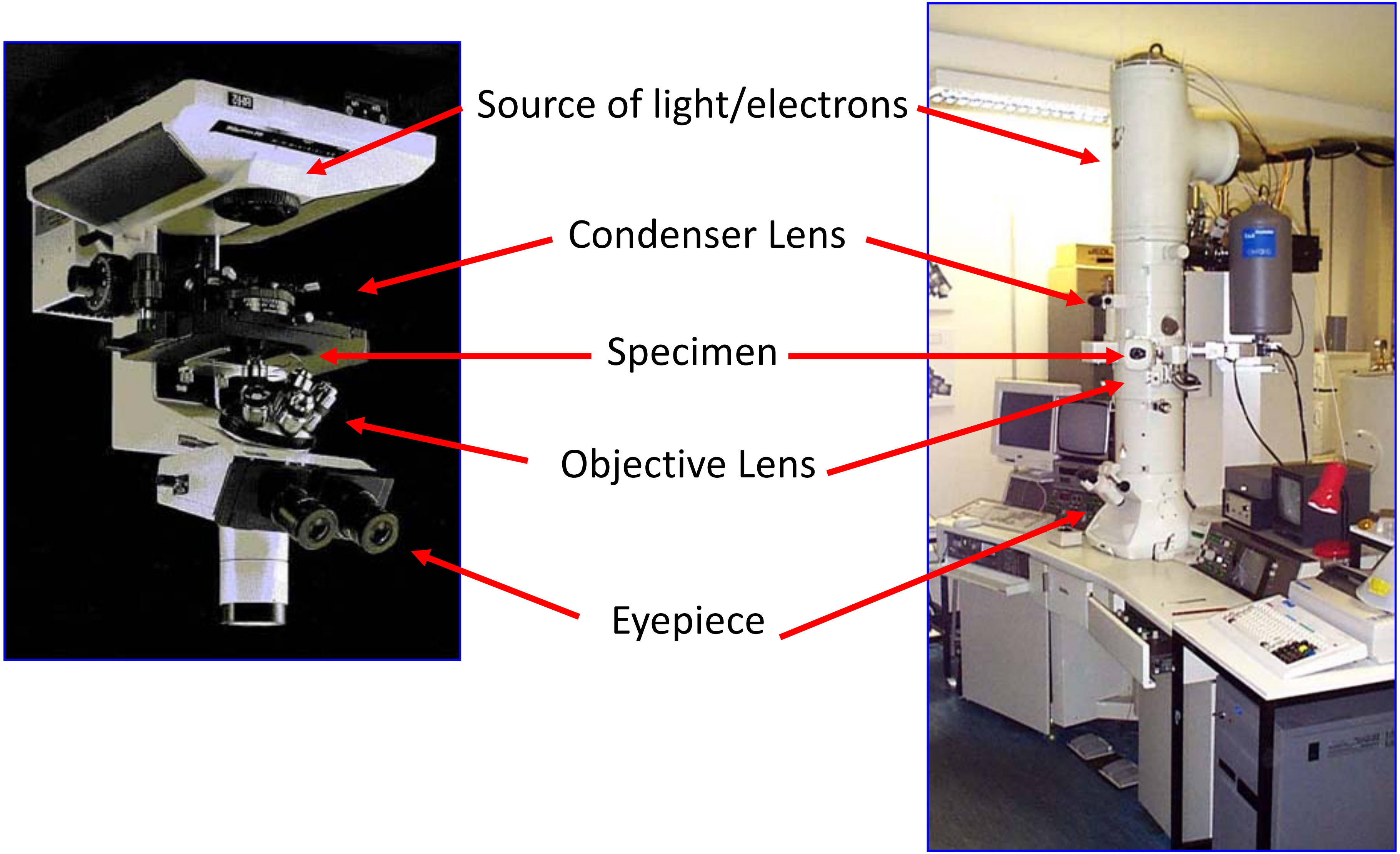

Interfacing of TEM and Ion Beam

University of Huddersfield

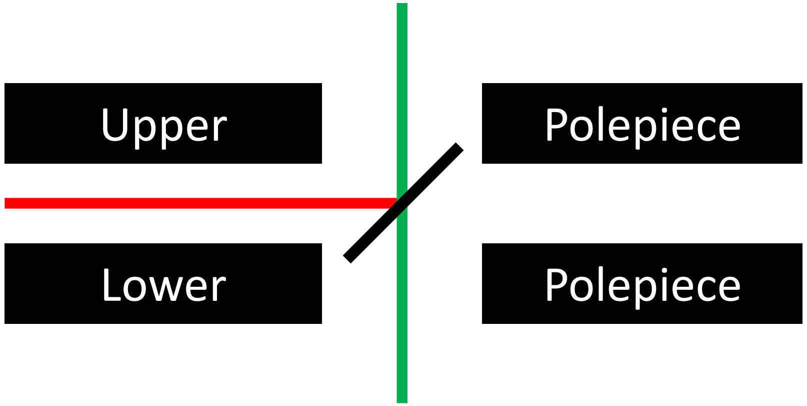

Side entry through polegap

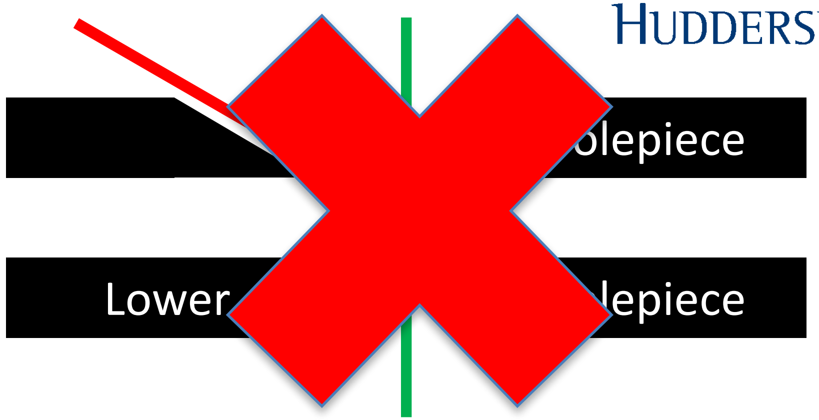

Bore through upper objective polepiece

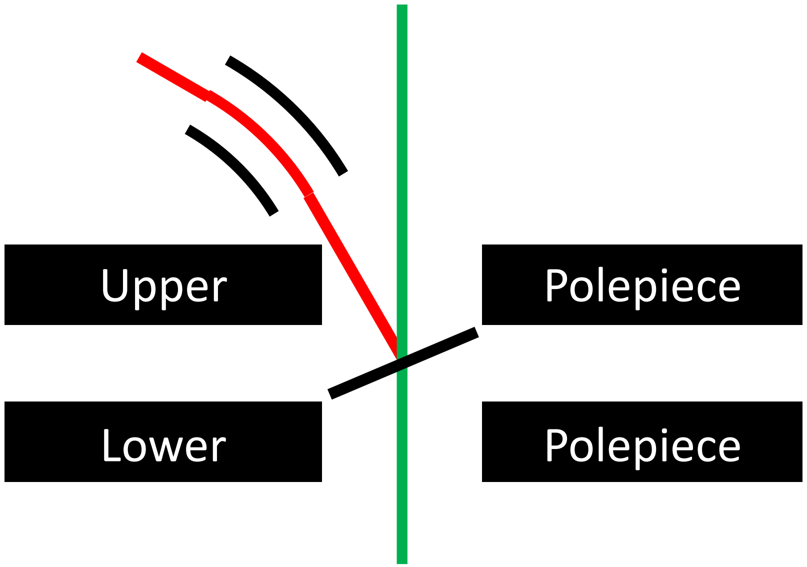

Electrostatic deflection inside TEM

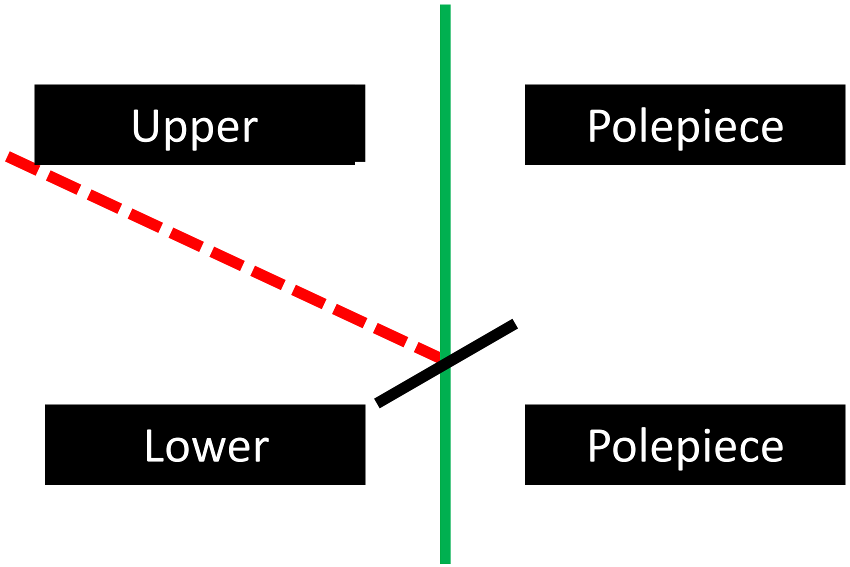

Possibilities offered by larger polegap

Interfacing of TEM and Ion Bea

University of HUDDERSFIELD

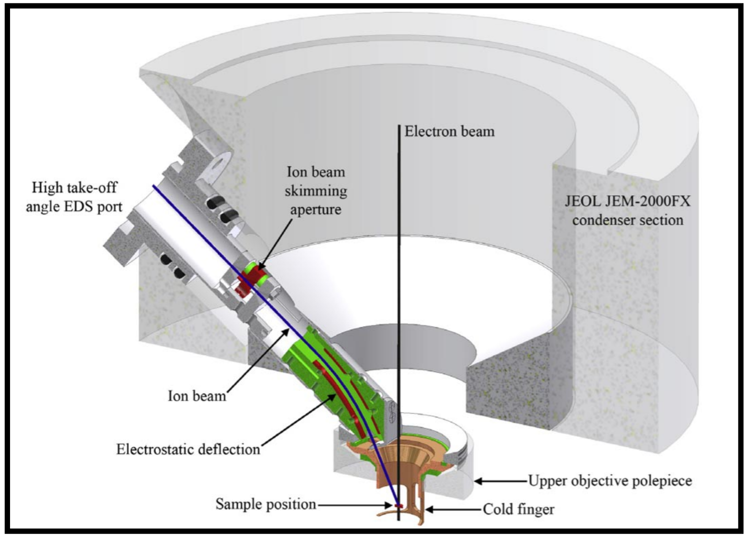

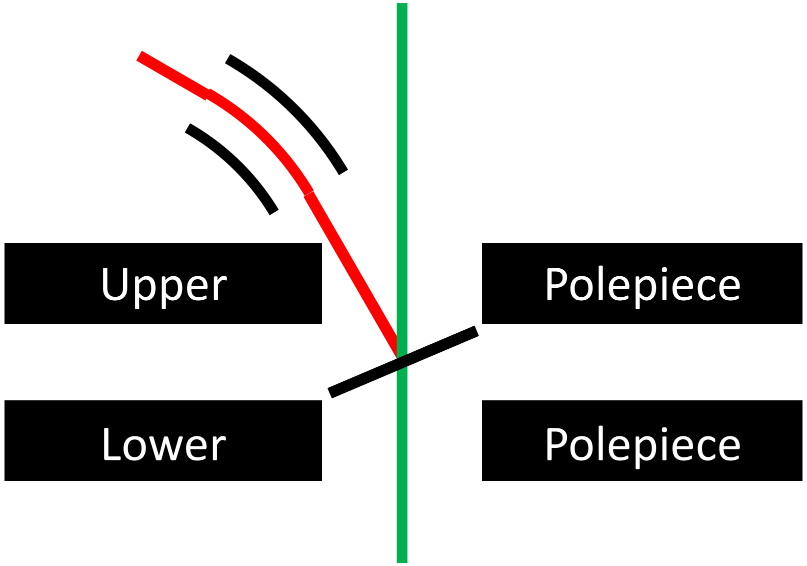

Electrostatic deflection inside TEM

MIAMI-1

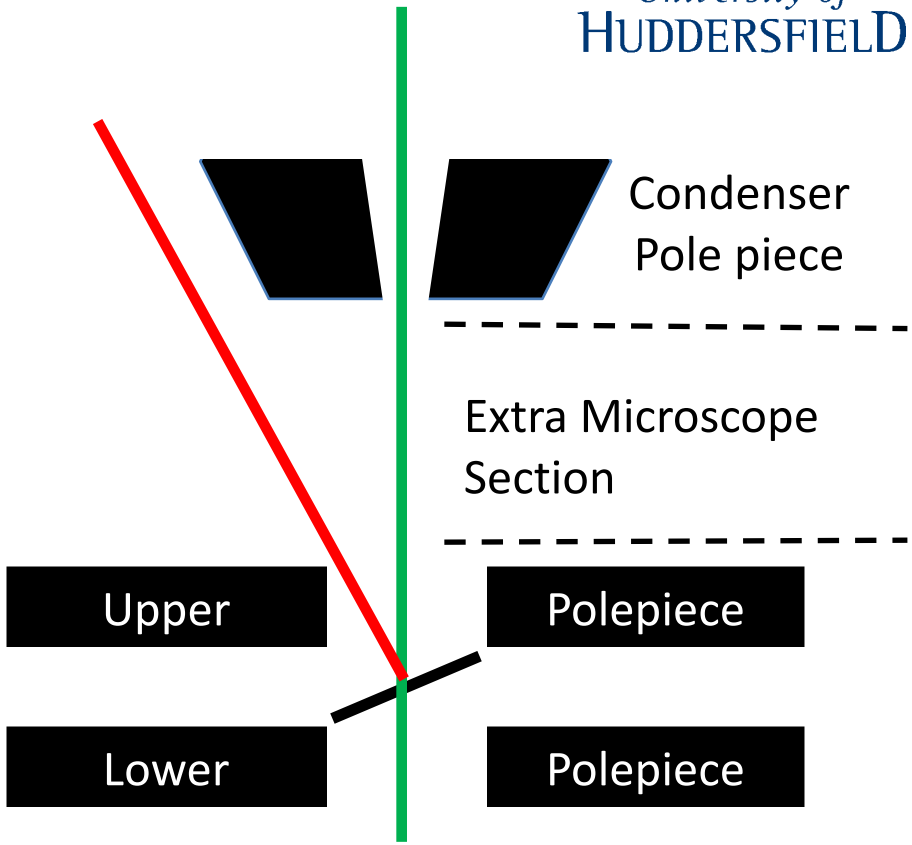

Direct line-of-sight to specimen
over top of upper objective polepiece

MIAMI-2

Interfacing of TEM and Ion Beam

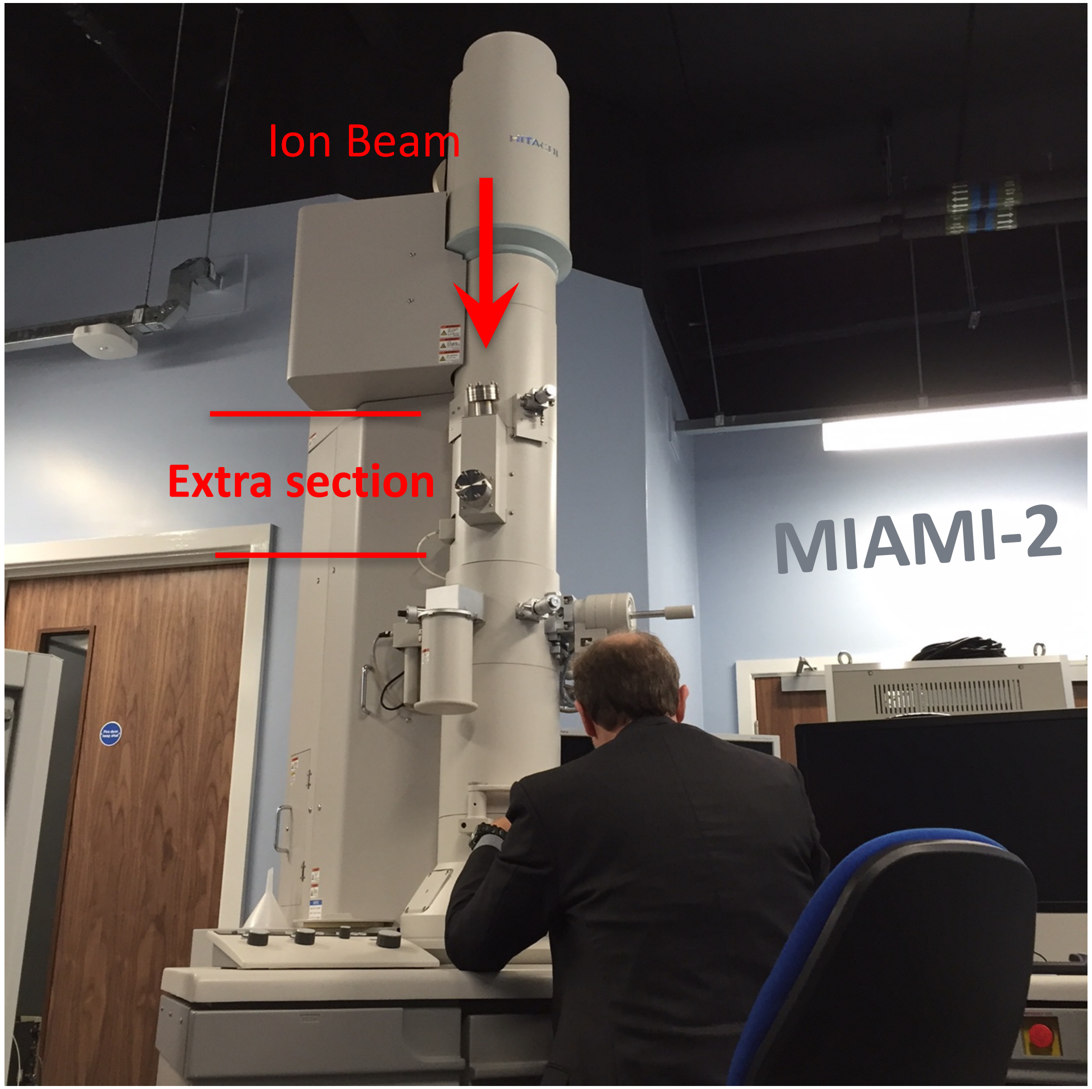

MIAMI*-1 Facility

*Microscope & Ion Accelerator for Materials Investigations

University of HUDDERSFIELD

Specifications	
TEM	JEOL JEM-2000FX
e-Beam Accelerating Voltage	80 to 200 kV
Ion Beam Accelerating Voltage	1 to 100 kV
Ion Species	Most ions from H to W at all energies (limited by bending magnet)
Ion Flux	Fluxes of up to 1.5×10^{14} cm^{-2} s^{-1} for 6 kV He (for example)
Angle between Ion and Electron Beams	30°
Temperature	100 to 380 K or RT to 1270 K
Image Capture	Gatan ES500W Wide Angle CCD Gatan Orius SC200 (4 Megapixels)

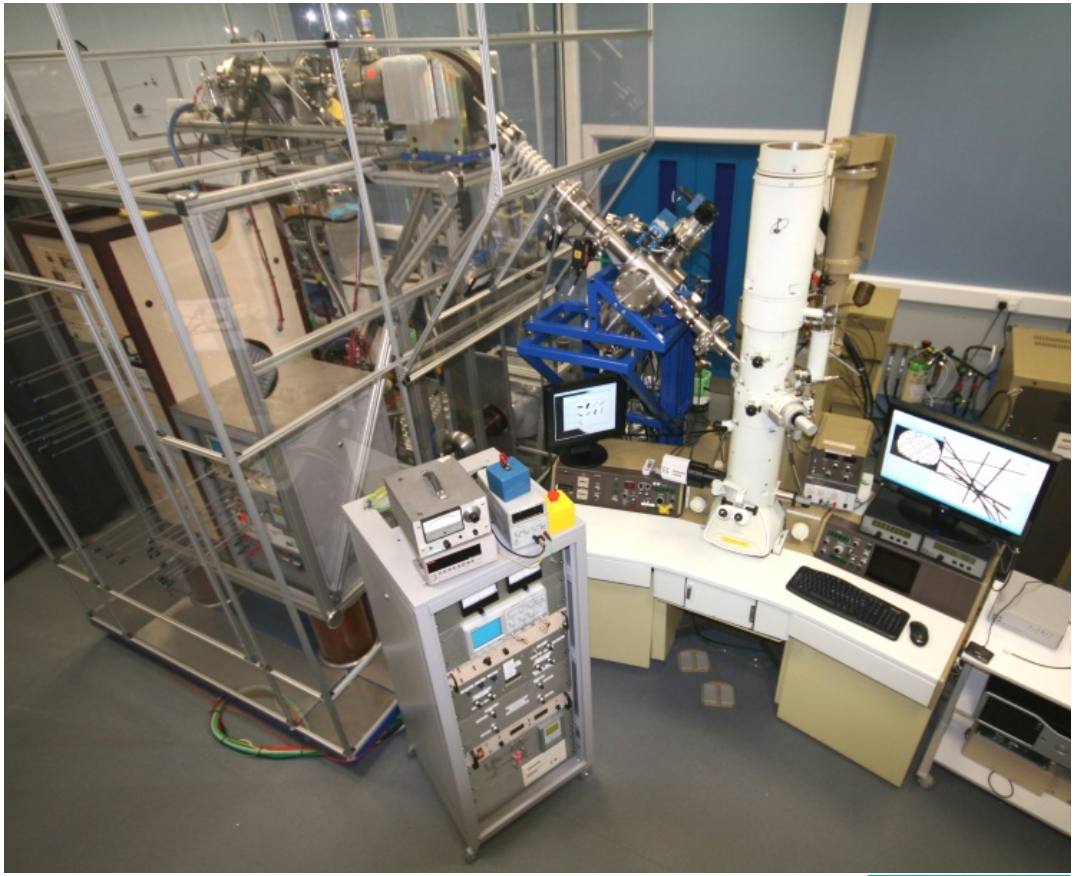

EPSRC

MIAMI*-2

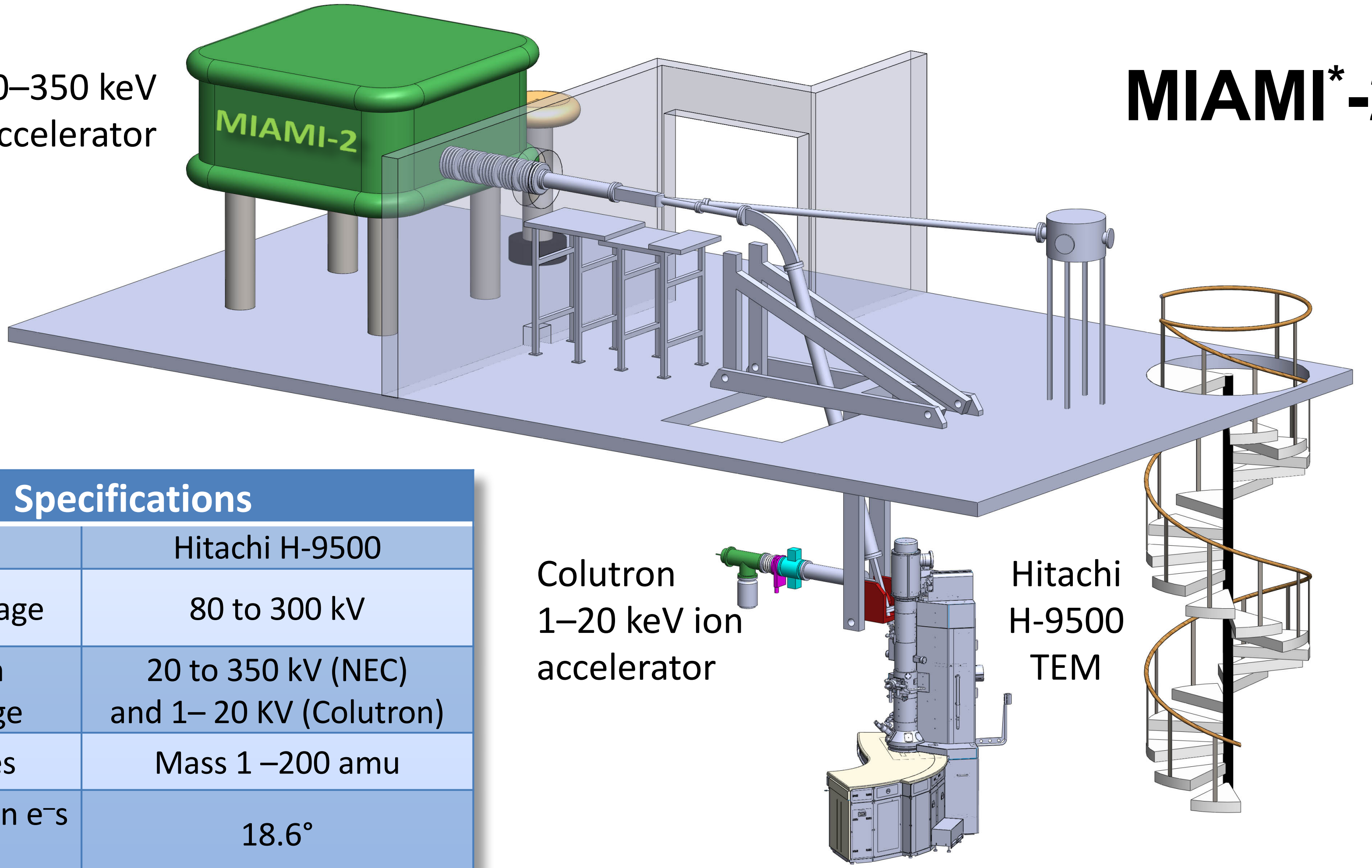

Specifications	
TEM	Hitachi H-9500
e-BeamVoltage	80 to 300 kV
Ion Beam Acc. Voltage	20 to 350 kV (NEC) and 1– 20 KV (Colutron)
Ion Species	Mass 1 –200 amu
Angle between e^{-}s & ions	18.6°
Environment	Temp: 100 to 1570 K Gas injection system
Image Capture	Gatan OneView 25 fps 4096x4096 px 300 fps 512x512 px
Analysis	EELS (Gatan Imaging Filter) and EDS
Tomography	Tomography holder and software

EPSRC

In-Situ Studies

Semiconductors

Formation Amorphous Zones in Silicon by Heavy-ion Impacts

Structure factor contrast

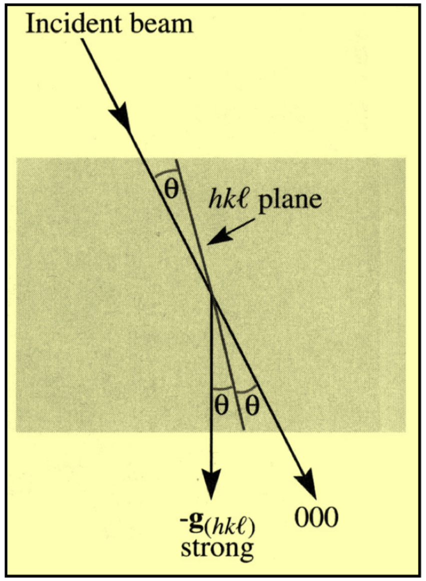

Two beam conditions

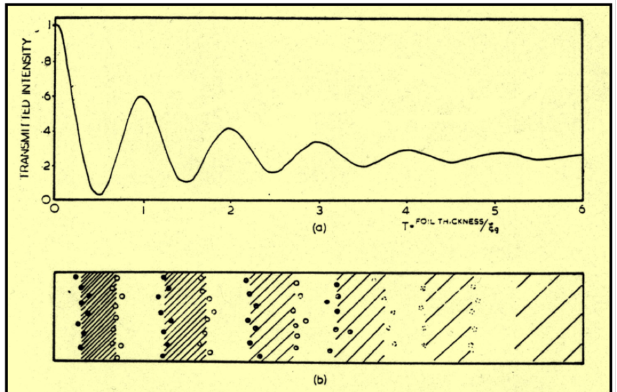

Diagram showing transmitted intensity oscillation with depth (5 (a)) and the positions of maximum visibility of particles by structure factor contrast (5 (b)). The position of light and dark particle images corresponds to $\xi_g > \xi_g'$. Light and dark images are reversed when $\xi_g < \xi_g'$

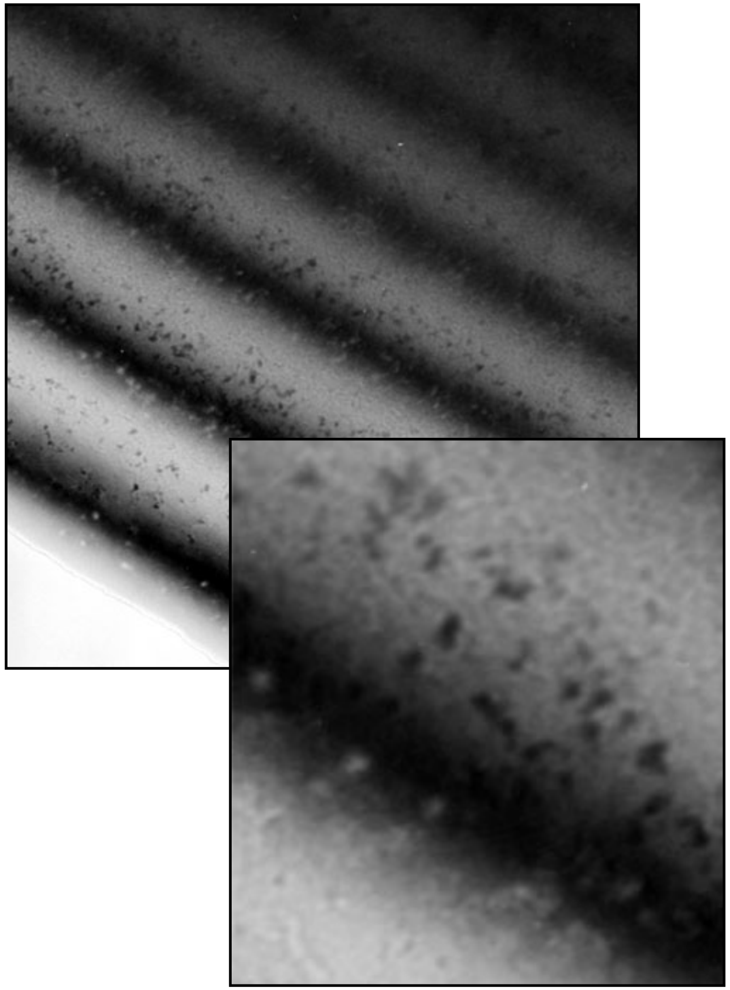

M. F. Ashby and L. M. Brown, *Philosophical Magazine* **8** (1963) 1649.

University of HUDDERSFIELD

Formation Amorphous Zones in Silicon by Heavy-ion Impacts

Recorded using a 100 keV electron beam.

No amorphisation is observed when using a 300 keV electron beam.

In this case amorphous zone, if formed, disappears in less than the time to record one video frame. (1/30th second).

Electrons acting as Kurt's "eraser"?

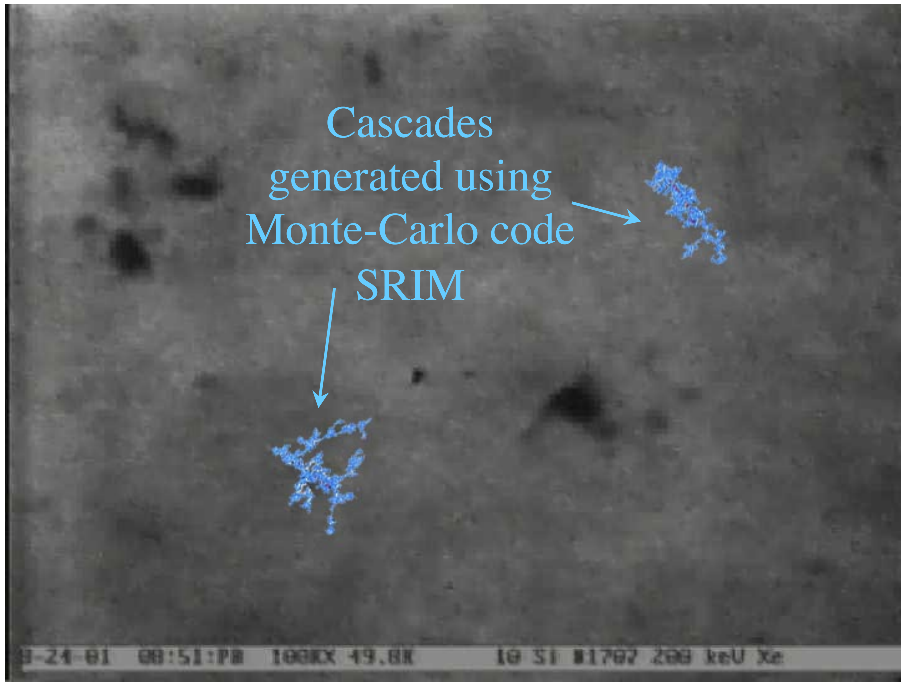

Width of image 110 nm

Direct impact amorphisation as discussed by Kurt Sickafus this morning. Literally "black spots" in this case!

Specimen irradiated with 200 keV Xe ions

Experiment conducted at the IVEM Facility at Argonne National Laboratory

S.E. Donnelly, R.C. Birtcher, V.M. Vishnyakov and G.Carter, Appl. Phys. Lett. **82** (2003) 1860

University of HUDDERSFIELD

He Irradiation of Silicon Trilayer — $Si/SiO_2/Si$

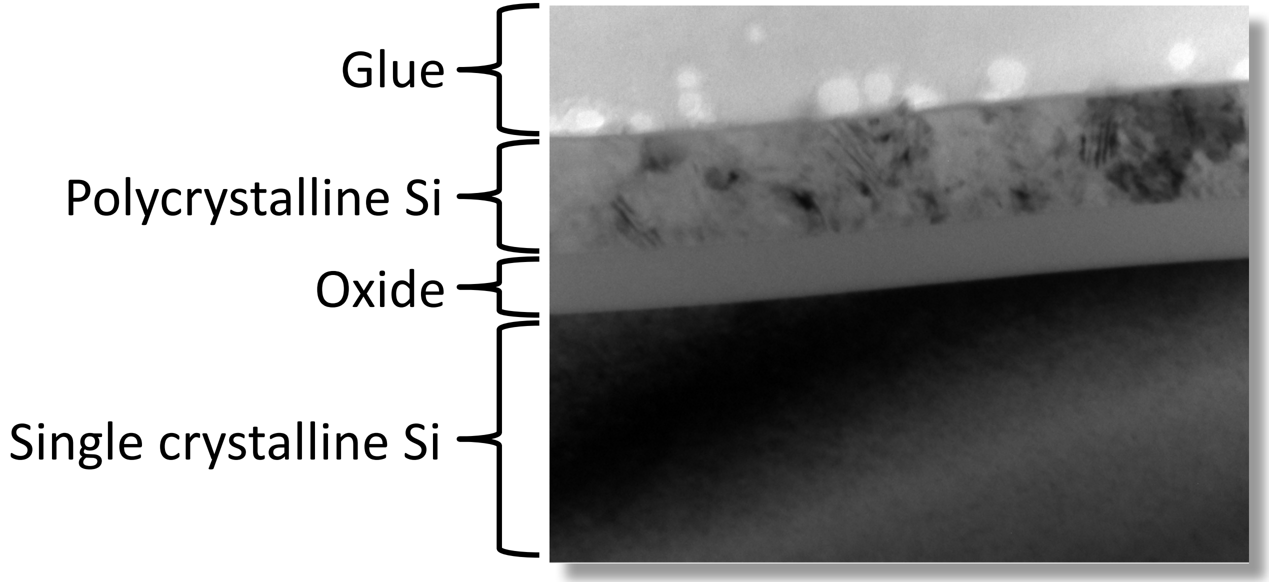

Image width = 550nm

Experiment to compare the development of helium bubbles in monocrystalline and polycrystalline silicon.

He-irradiation of Si/SiO_2

Develops a high degree of porosity

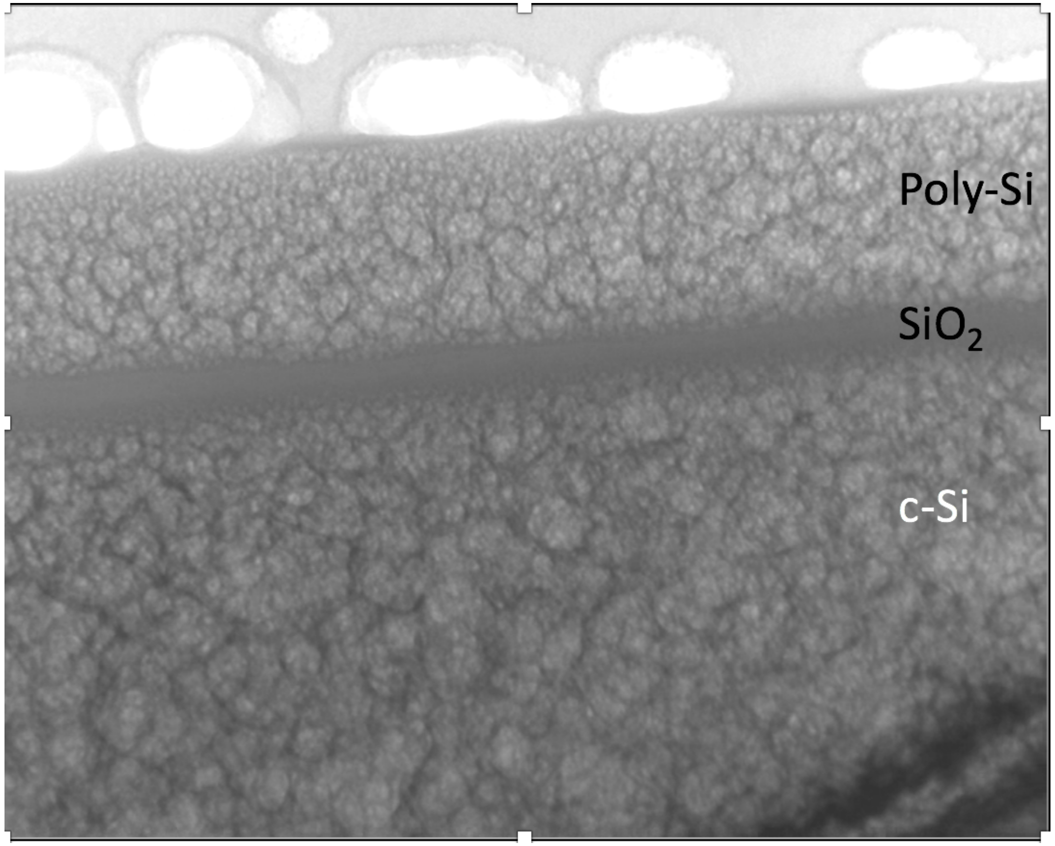

Image width ≈ 550 nm

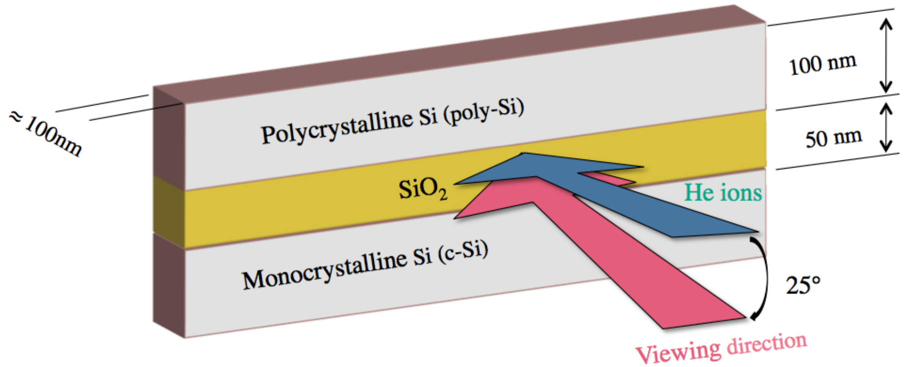

Ion energy: 6 keV

Final fluence: ≈ 5 x 10^{17} ions/cm^2

Flux: ≈ 3 x 10^{13} ions/cm^2/s

K. J. Abrams, J. A. Hinks, C. J. Pawley, G. Greaves, J. A. van den Berg D. Eyidi, M. B. Ward, S. E. Donnelly.
J. Appl. Phys. **111,** 083527 (2012); doi: 10.1063/1.4705450

University of HUDDERSFIELD

In-Situ Studies

Nanostructures

Heavy Ion Impacts on Au foil

University of HUDDERSFIELD

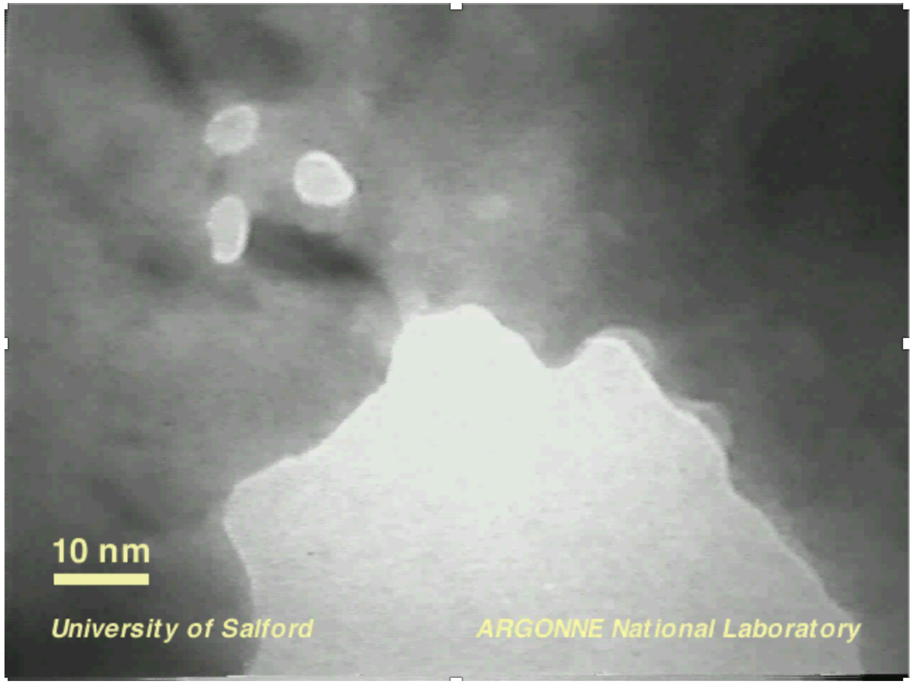

Holes caused by individual ion impacts

20 nm

Individual 200 keV Xe ions impacting on a thin gold film
NB: specimen is at room temperature.

R C Birtcher and S E Donnelly, Phys. Rev. Letters **77** 21 (1996) 4374

Heavy Ion Impacts on Au Nanorods

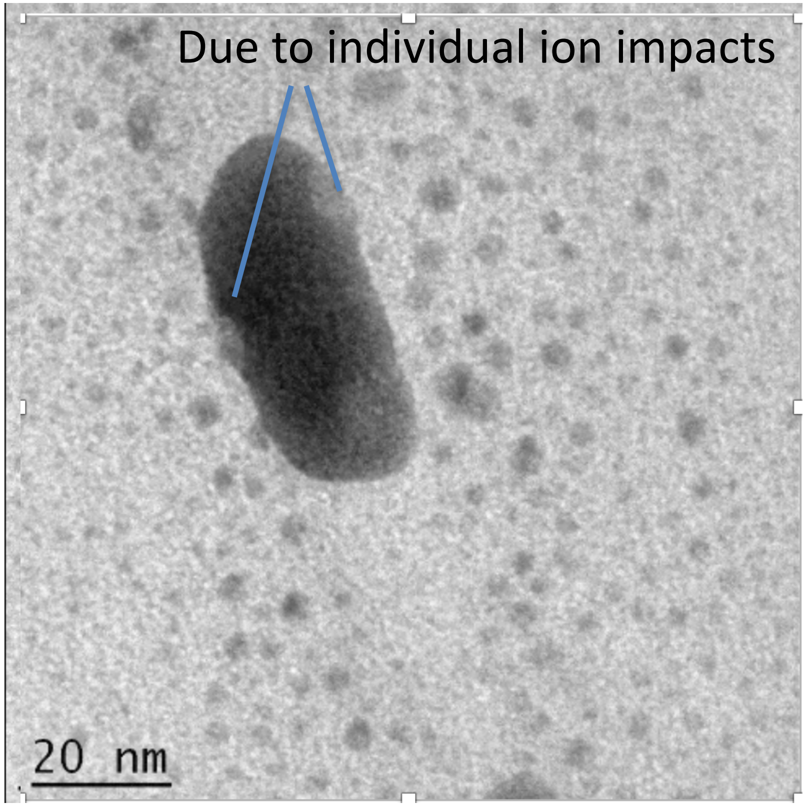

Monocrystalline nanorod on Formvar film.
80 keV Xe ions. Flux ≈ 2.1×10^{11} ions/cm^2/s.
Temperature ≈ 20°C. Video playback rate = x 8

The Au nanorod remains solid at all times (as indicated by diffraction contrast); however, localised melting due to the thermal spike induced by each impact together with flow/surface tension processes modify shape of nanorod. There is also a decrease in volume resulting from (enhanced sputtering yield).

(The small particles are Au grains growing as a result of sputter-deposition of Au on the Formvar film).

G. Greaves, J. A. Hinks, P. Busby, N. J. Mellors, A. Ilinov, A. Kuronen, K. Nordlund, and S. E. Donnelly, *Phys. Rev. Lett*. **111** (2013) 065504

Molecular Dynamics Simulations

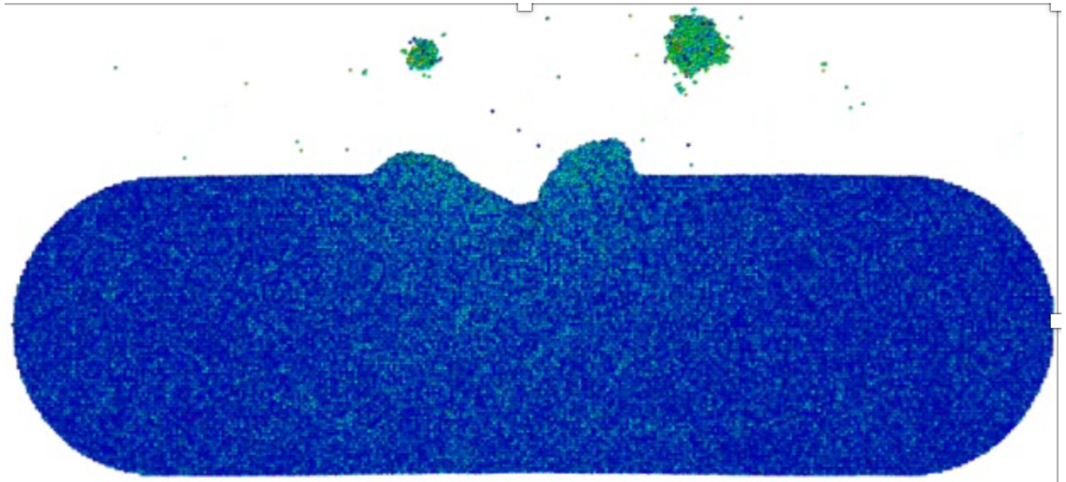

"Explosive" cluster emission is additional to ballistic and thermal components of sputtering yield

Sputtering yield from impact shown: S=2560 atoms/ion

About 100 atoms sputtered due to "normal" ballistic and thermal processes – the rest due to cluster emission.

MD simulations by Kai Nordlund's group, University of Helsinki

Molecular Dynamics Simulations

University of HUDDERSFIELD

Sputtering yield from this simulated impact:

S =2560

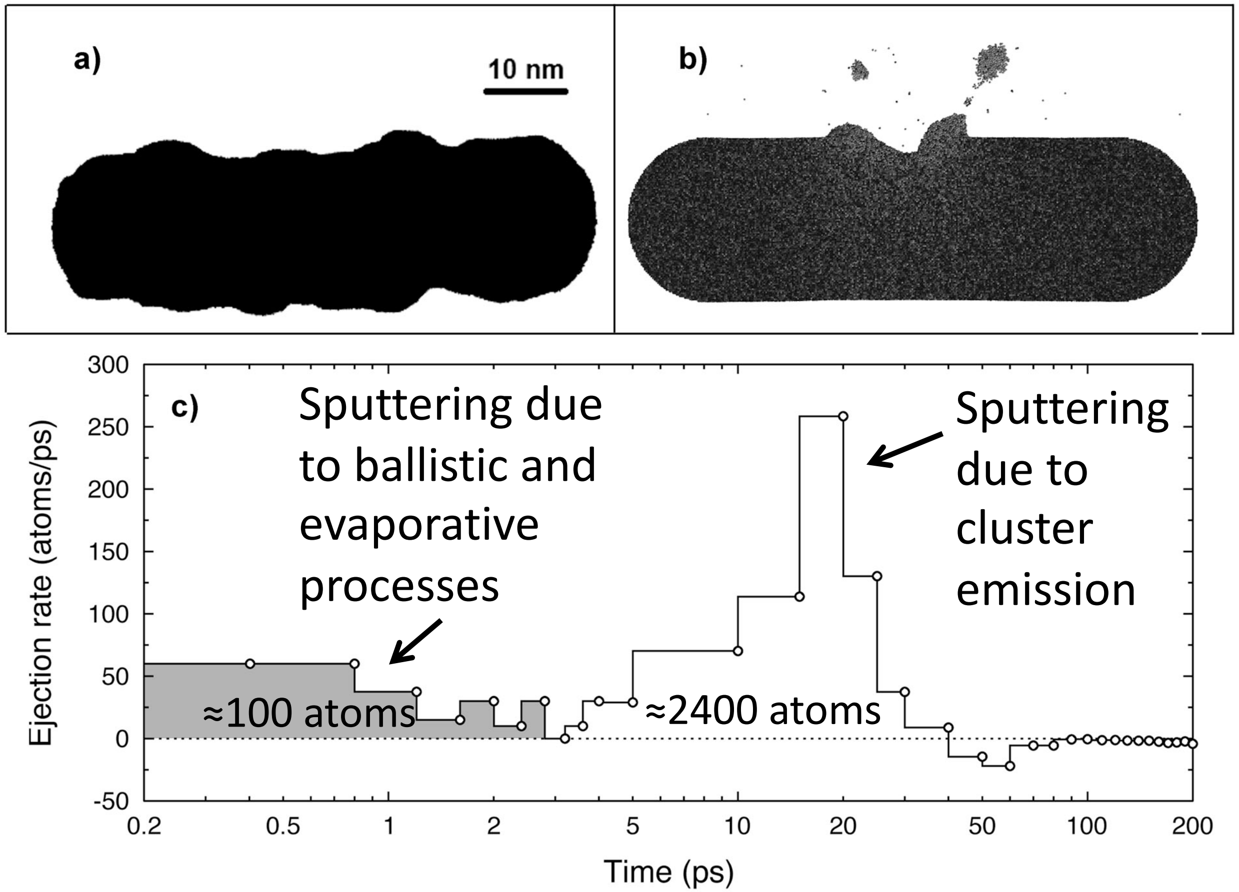

Average sputtering yield from 30 simulated impacts:

S =1005

Results of MD simulations of 80 keV Xe ions on an Au nanorod: a) silhouette of the nanorod following 30 ion impacts; b) image at 80 ps following a single ion impact showing a crater and ejected nanoclusters; c) plot of ejection rate (atoms/ps) as a function of time for a single 80 keV Xe ion impact. The shaded area indicates the contribution from ballistic and evaporative processes. Each point indicates the mean ejection rate for the period since the previous point. The negative ejection values around 50 ps result from atoms evaporated from the clusters being redeposited on the nanorod.

Ion-Beam-Induced Bending of Nanowires

- Phenomenon reported in literature mainly in semiconductors nanowires (Si, Ge, GaAs, ZnO) but also Pt and W
- Various models have been proposed in the literature but the prevailing explanation is volume change due to damage accumulation
- Other mechanisms have been suggested including electronic-energy loss, thermal expansion and sputtering
- A general trend is observed that irradiation conditions with shallower damage profiles lead to bending away from the ion beam and deeper profiles cause bending towards the ion beam.

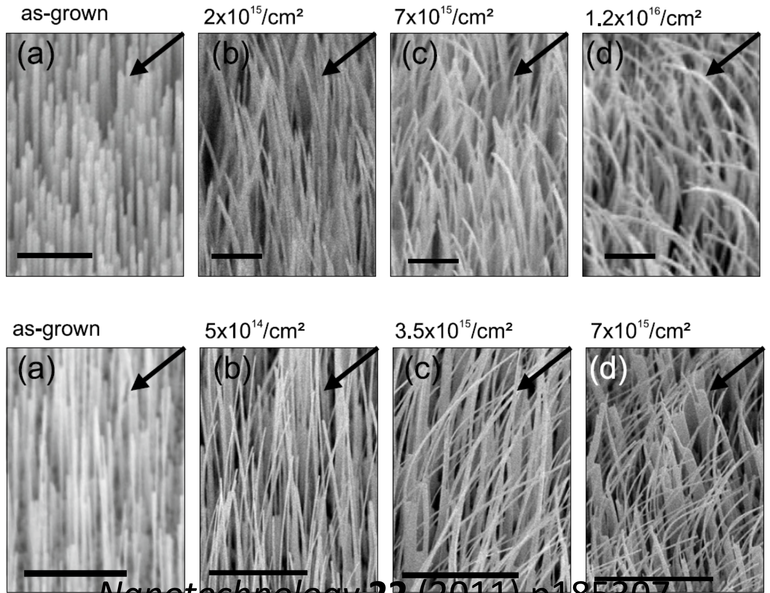

Nanotechnology **22** (2011) p185307

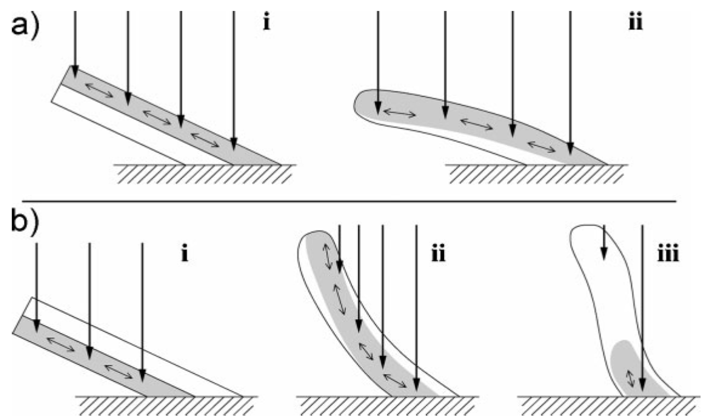

Small **22** (2009) p2576

Ion-Beam-Induced Bending of Nanowires

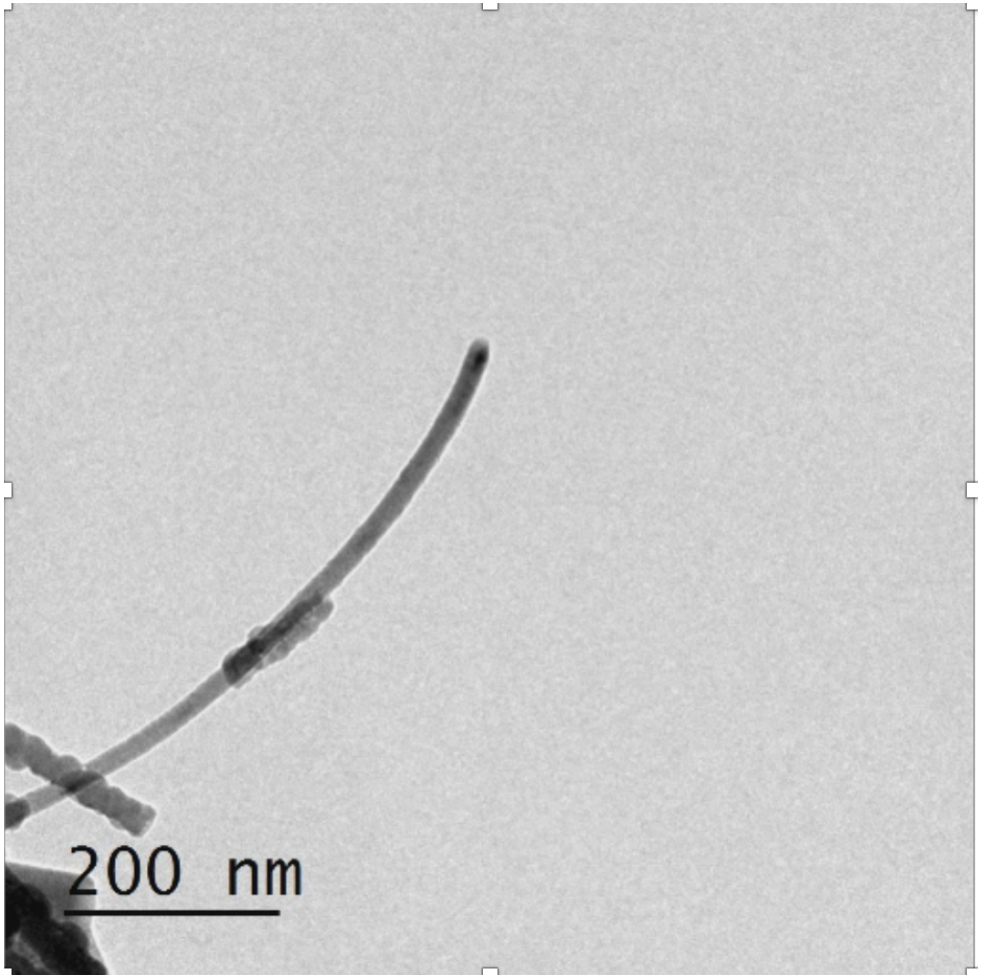

7 keV Xe^{+} irradiation of silicon nanowire at RT

End fluence = 1.2×10^{14} ions.cm^{-2}

Work by I. Hanif, PhD student, University of Huddersfield.

In-Situ Studies

Materials in Space

Xe Irradiation of Nanodiamonds

University of HUDDERSFIELD

Meteoric nanodiamonds are observed to contain noble gases (particularly Xe) probably implanted by shock waves in supernovae explosions. In this context, we are interested in studying Xe ion irradiation of nanodiamonds .

Frame width 75 nm

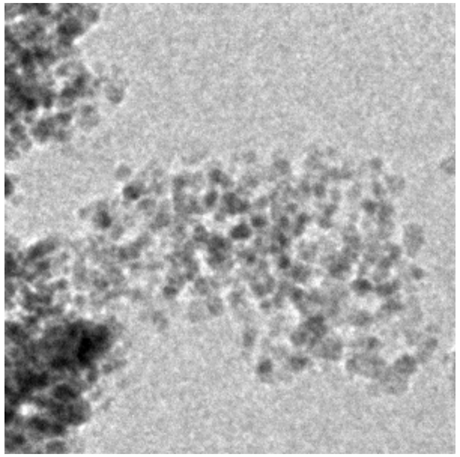

Before irradiation

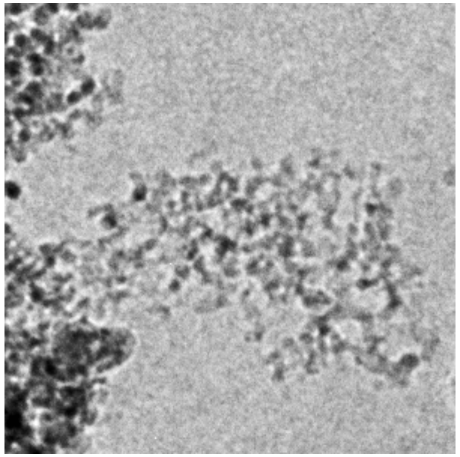

After irradiation

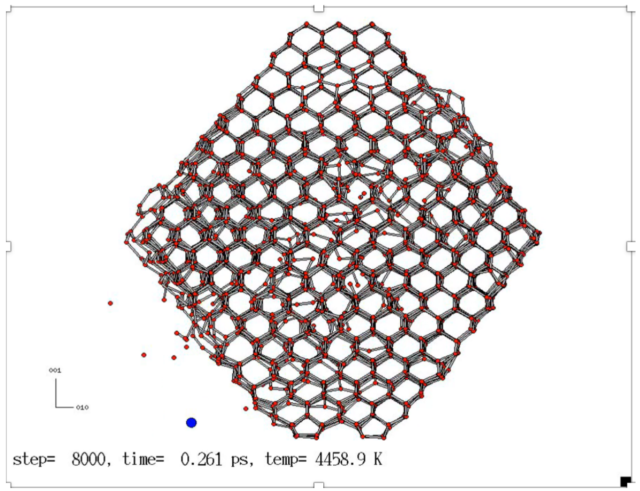

MD simulation by N. Marks

Irradiation of nanodiamonds with
6 keV Xe ions. Fluence = 6.5 x 10^{15} ions/cm^2

Reduction in size of nanodiamonds

Ongoing collaboration with A.A. Shiryaev, Institute of Physical Chemistry and Electrochemistry, Russia and N. Marks, Curtin University, Australia

Nuclear Materials: Graphite

Radiation Damage in Graphite

Fundamentals of Nuclear Graphite (FUNGraph):

Work carried out as part of an EPSRC consortium grant awarded to the universities of Sussex, Salford, Nottingham, Manchester, Leeds and Huddersfield.

The project aimed to understand the behaviour of nuclear graphite under neutron irradiation at elevated temperatures.

Radiation Damage in Graphite

Xe damage profile is strongly peaked towards bottom of film leading to greater basal-plane contraction in the bottom of the film than in the top

This then results in dislocation formation followed by ridge formation.

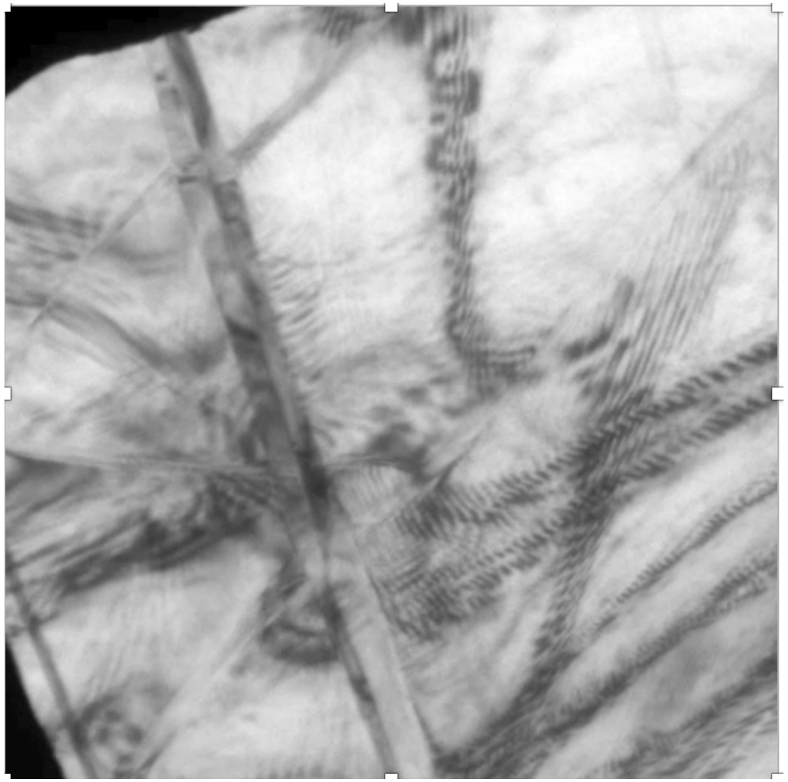

Frame width = 3.65 µm

Room-temperature irradiation with 60 keV Xe ions with a flux of10^{10} ions/cm^2/s. Video playback rate = x 8

J.A. Hinks, S.J. Haigh, G. Greaves, F. Sweeney, C.T. Pan, R.J. Young, S.E. Donnelly, Carbon **68** (2014) 273

Radiation Damage in Graphite

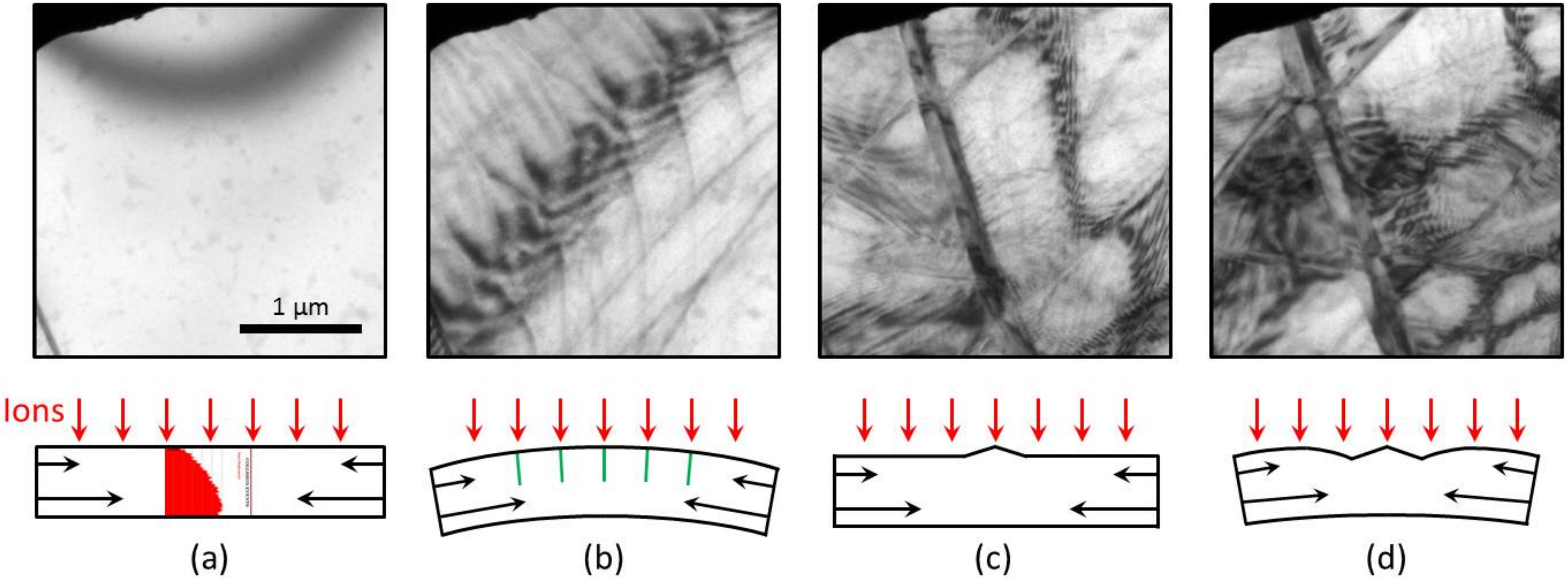

Point defect creation leads to stress build-up non-uniformly in film presumably due to contraction of basal planes occurring to a greater degree in the lower part of film

Propagation of basal-plane dislocations.

Ridge formation and cracking of film to form platelets/ grains.

Continued deformation of platelets leading to further ridge/crack formation

Deformation under ion irradiation

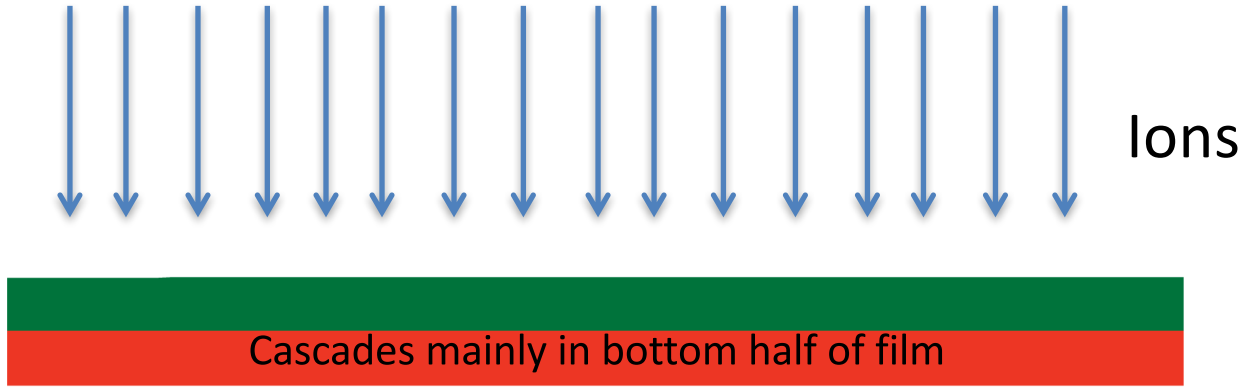

Deformation under ion irradiation

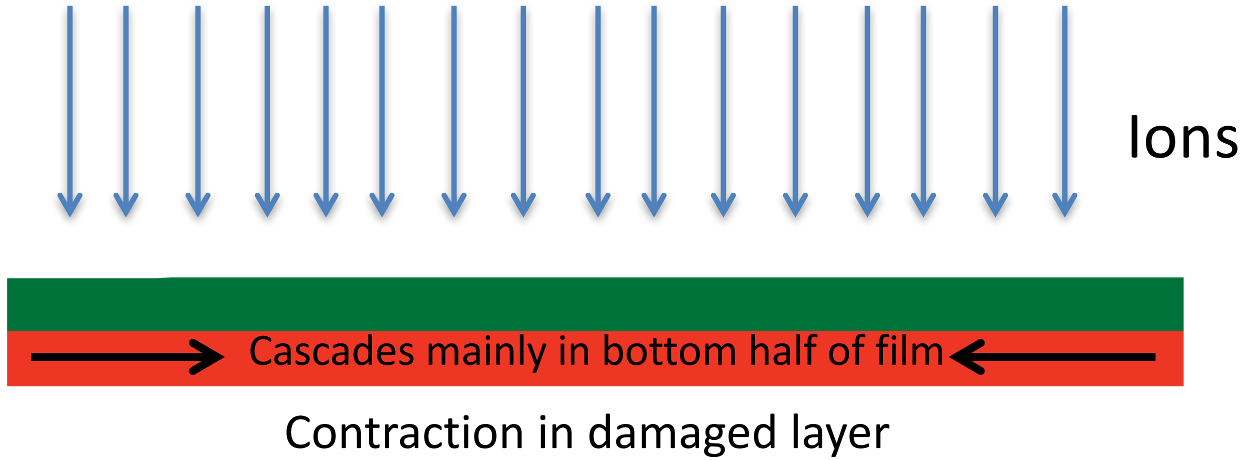

Deformation under ion irradiation

University of HUDDERSFIELD

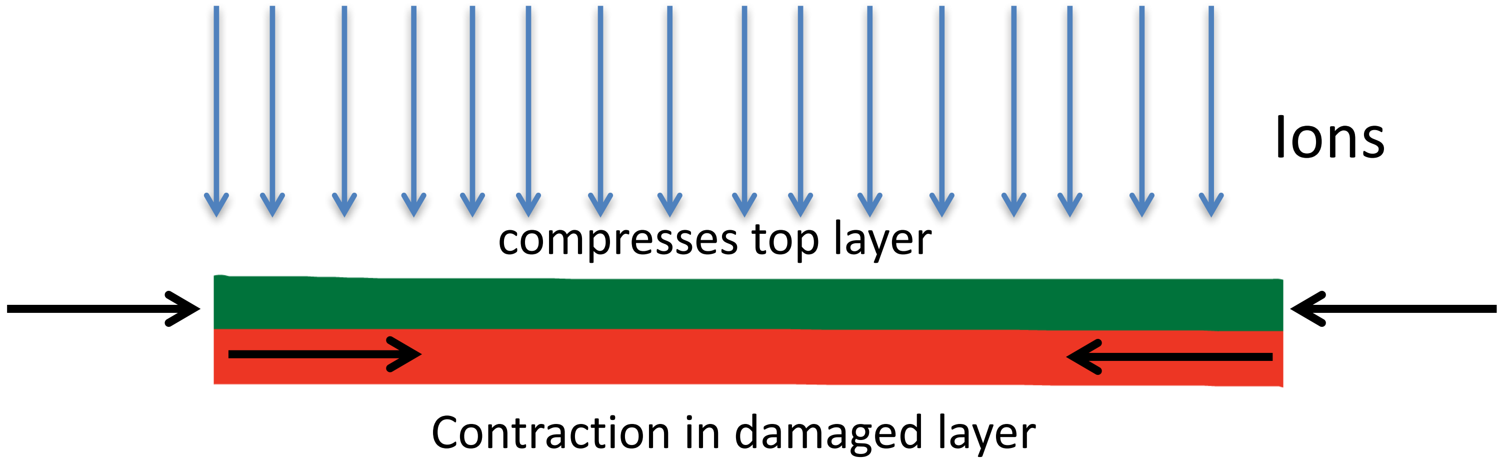

Deformation under ion irradiation

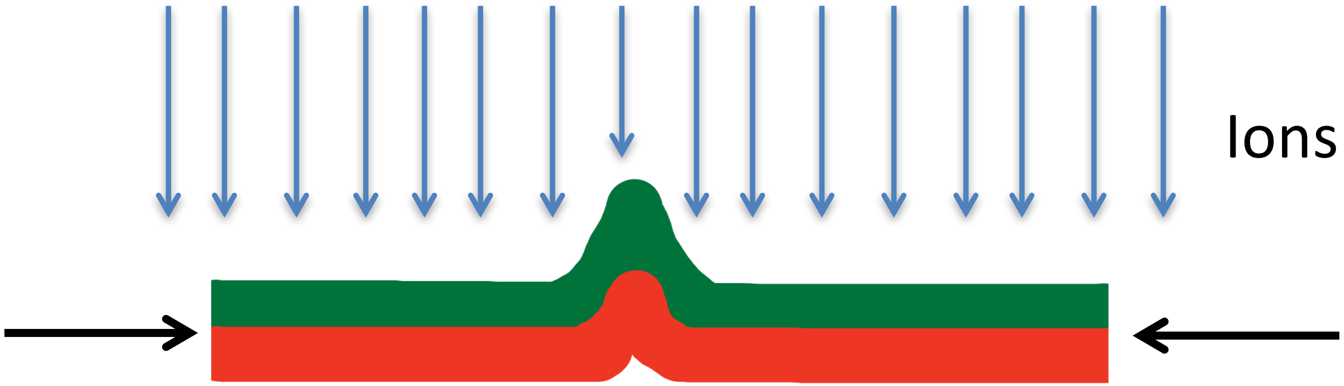

Deformation occurs. Extra volume in top layer is accommodated in kink

Radiation Damage in Graphite

Experiments have also been performed at 100 and 673 K (400°C) showing same effects.
Note that both interstitials and vacancies are both expected to be immobile at 100 K.
Suggests that process is NOT driven by point defect creation, migration and agglomeration.

$E_{\mathrm{m,V}} \cong 1.0$ eV
$E_{\mathrm{m,I}} \cong 1.2$ eV
Computational Nanoscience (RSC Publishing, London 2011)

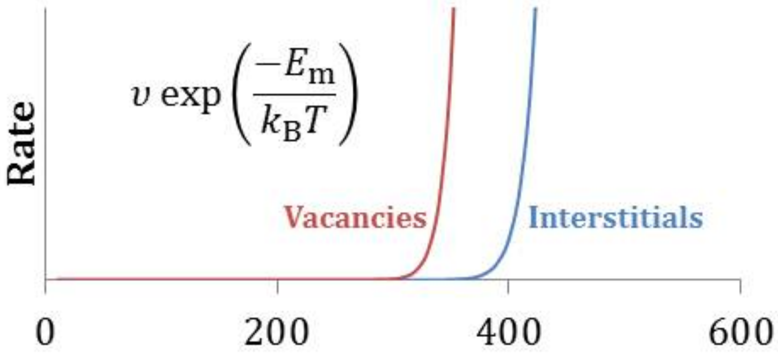

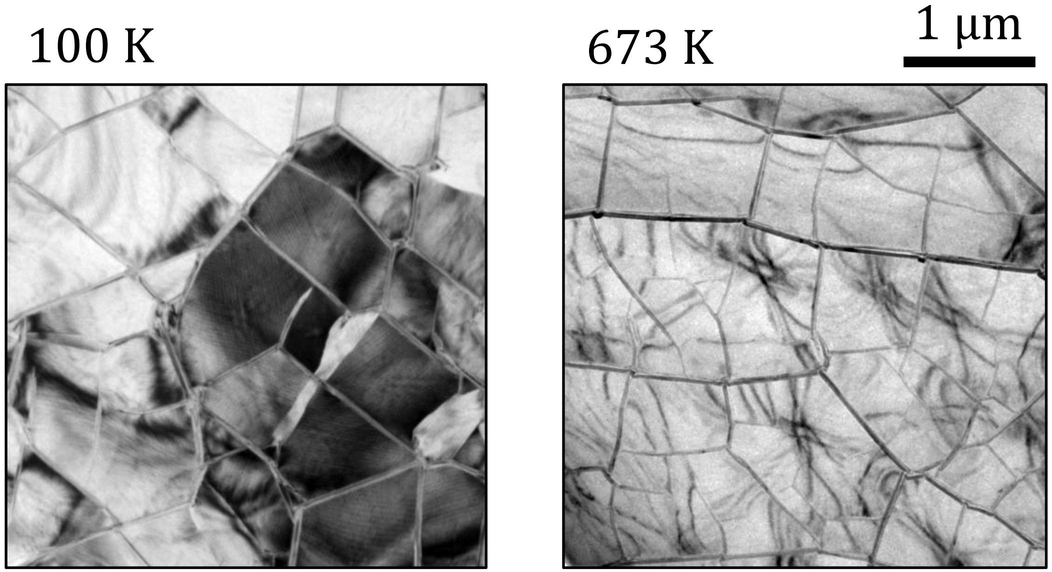

But how does contraction of basal planes occur?
Need agglomeration of vacancies (e.g. into line).

Mechanism for transformation of immobile point defects in dilute cascade into macroscopic deformation is not understood.

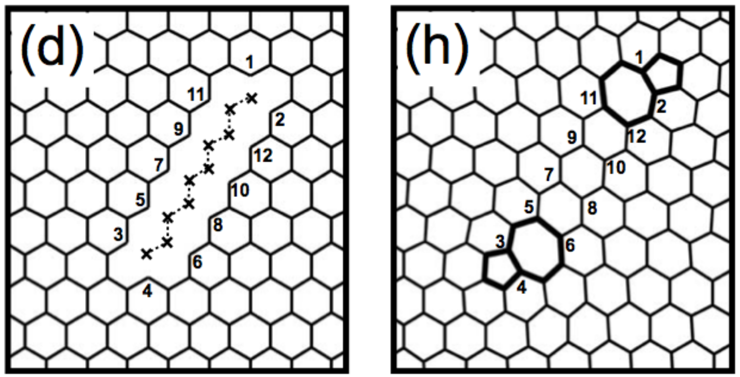

From B Wook Jeong, J Ihm and G-D Lee PRB **78**, 165403 2008

“He/DPA” Project

- To develop an understanding of the roles that displacement damage, helium content and temperature play in determining the defect morphology in a number of model structural nuclear materials, including Fe/Cr alloys, W and SiC.
- To develop an understanding of the roles that displacement damage, helium content, glass composition (specifically alkali content) have on defect morphology (particularly the development of helium bubbles) in alkali borosilicate, lanthanide borosilicate and aluminosilicate glasses with a view to being able to predict the defect structures that might be expected to develop in these glasses in geological disposal facilities.
- To study the role played by the ceramic/glass interface in the development of defect structures (particularly those related to helium bubbles) in model glass/ceramic wasteforms.

Structural Materials: Fission Reactors

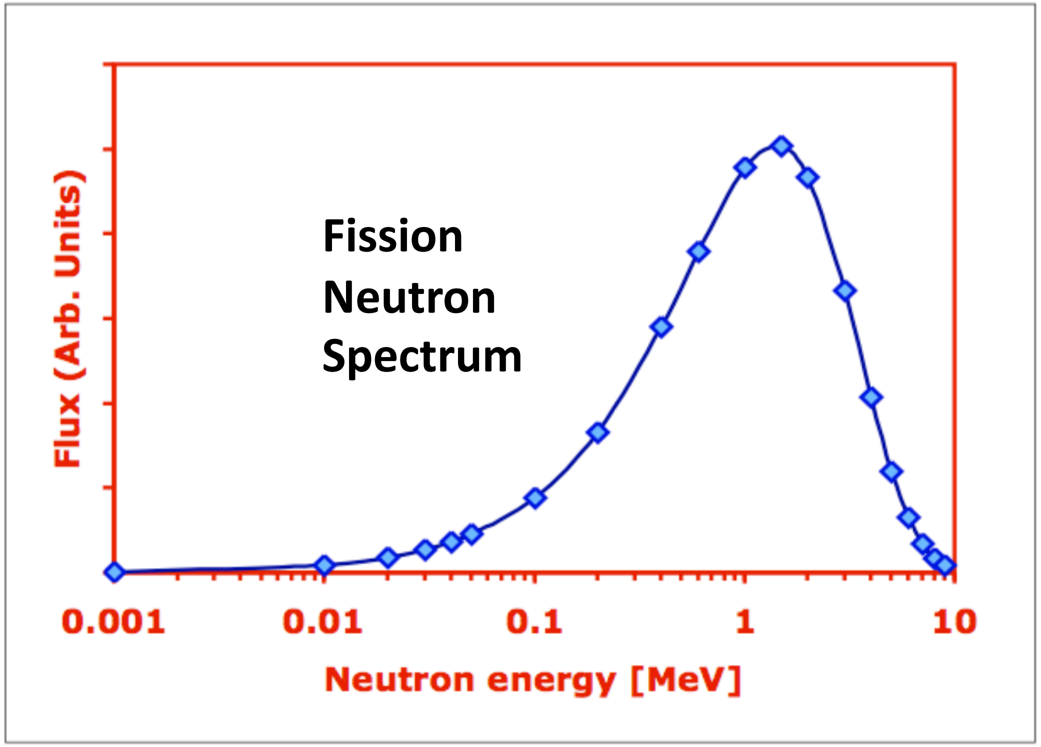

Max Energy Transfer from 1 MeV Neutron		
Element	Mass	E_{max} (keV)
Fe	56	69
W	184	21
Si	28	133
C	12	284

Maximum energy of primary knock-on (PKA)

Two important parameters to be simulated using ion beams: displacement damage and transmutation gas build-up, mainly He.

J. Watterson, https://indico.cern.ch/event/145296/contributions/1381141/attachments/136909/194258/lecture24.pdf

Structural Materials: Fusion

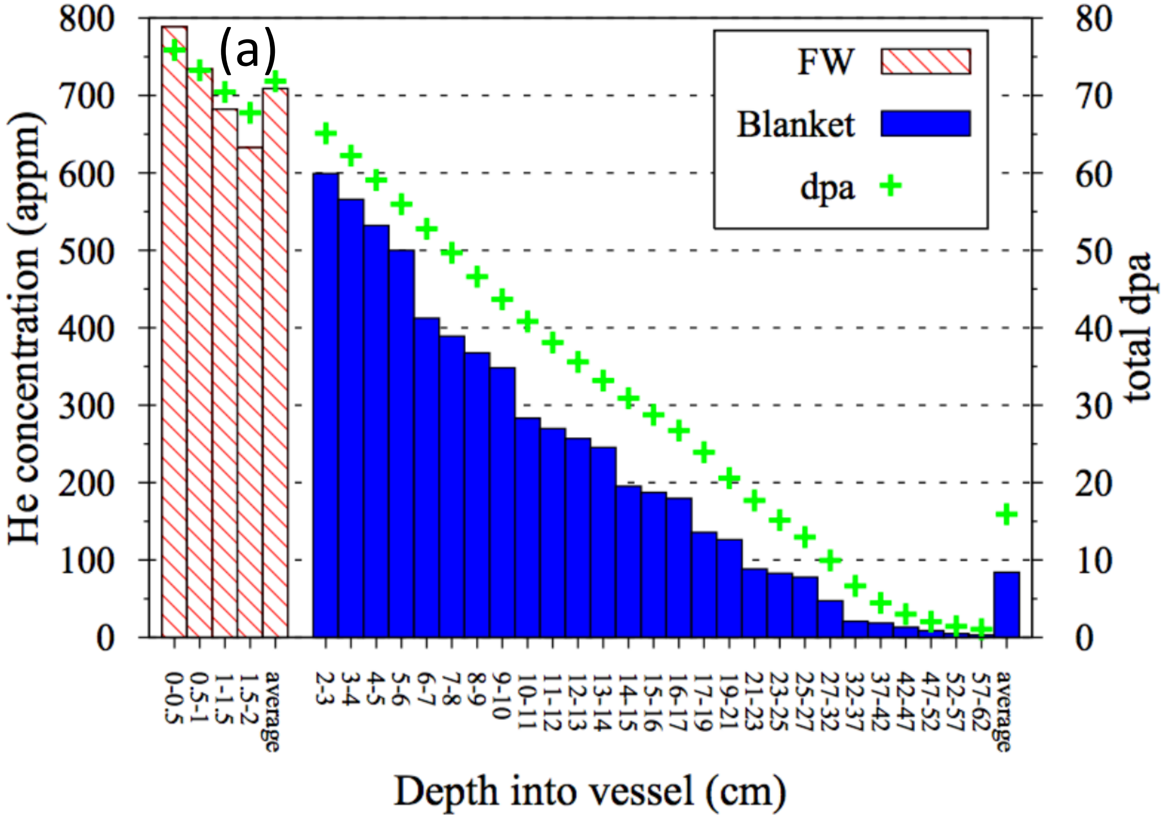

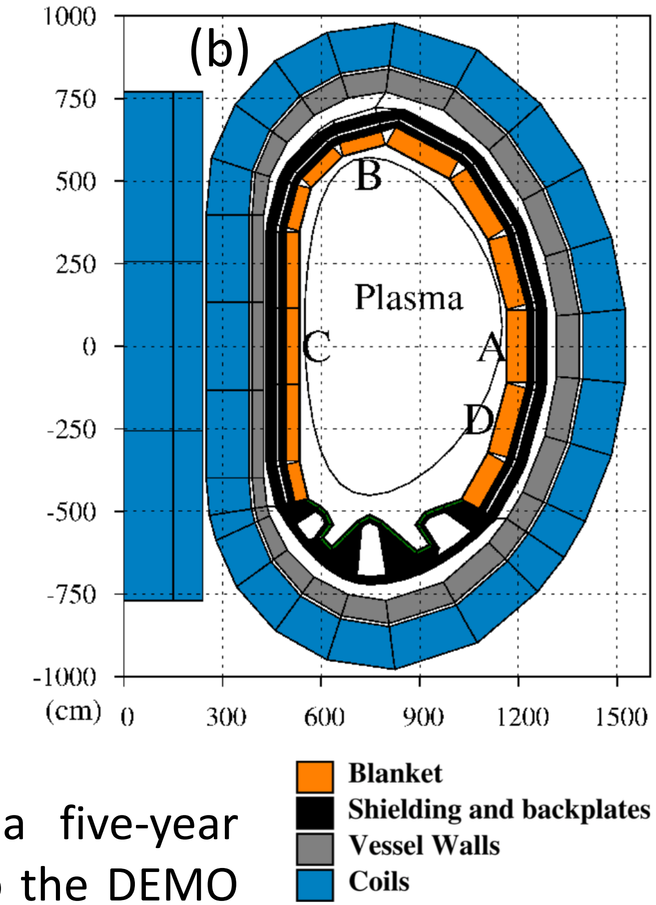

(a) Variation in He concentration in pure Fe after a five-year irradiation as a function of depth (from the plasma) into the DEMO vessel at (A) in figure (b). Also shown is the total dpa in pure Fe, evaluated by integrating the dpa rates over time, at each depth after five years.

Calculated He and DPA in DEMO Fusion Reactor

M.R. Gilbert, S.L. Dudarev, S. Zheng, L.W. Packer, and J.-Ch. Sublet, Nuclear Fusion, **52** (8), (2012)

Nuclear Wasteforms

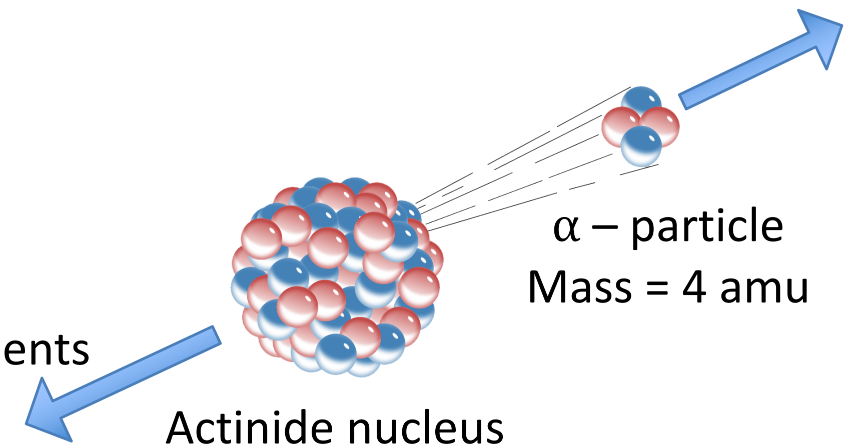

In wasteforms, after 500–1000 years, β-decay becomes negligible and damage is due to α-decay which may result in the build-up of both He and displacement damage, the former due to α-particles acquiring two electrons and coming to rest within the glass, the latter due to both the α-particle itself (energy 4.5– 5 MeV) and the recoiling heavy nucleus (energy 70–100 keV). These contribute approximately 1500 displacements (200 from the α-particle, 1300 from the recoiling nucleus) per decay event, yielding a (relatively) constant value of $R_{He/DPA}$ (ratio of He content to DPA) in the range 600–700 (appm He)/DPA.

He/DPA ratio available using 40–100 keV He irradiation of TEM foil

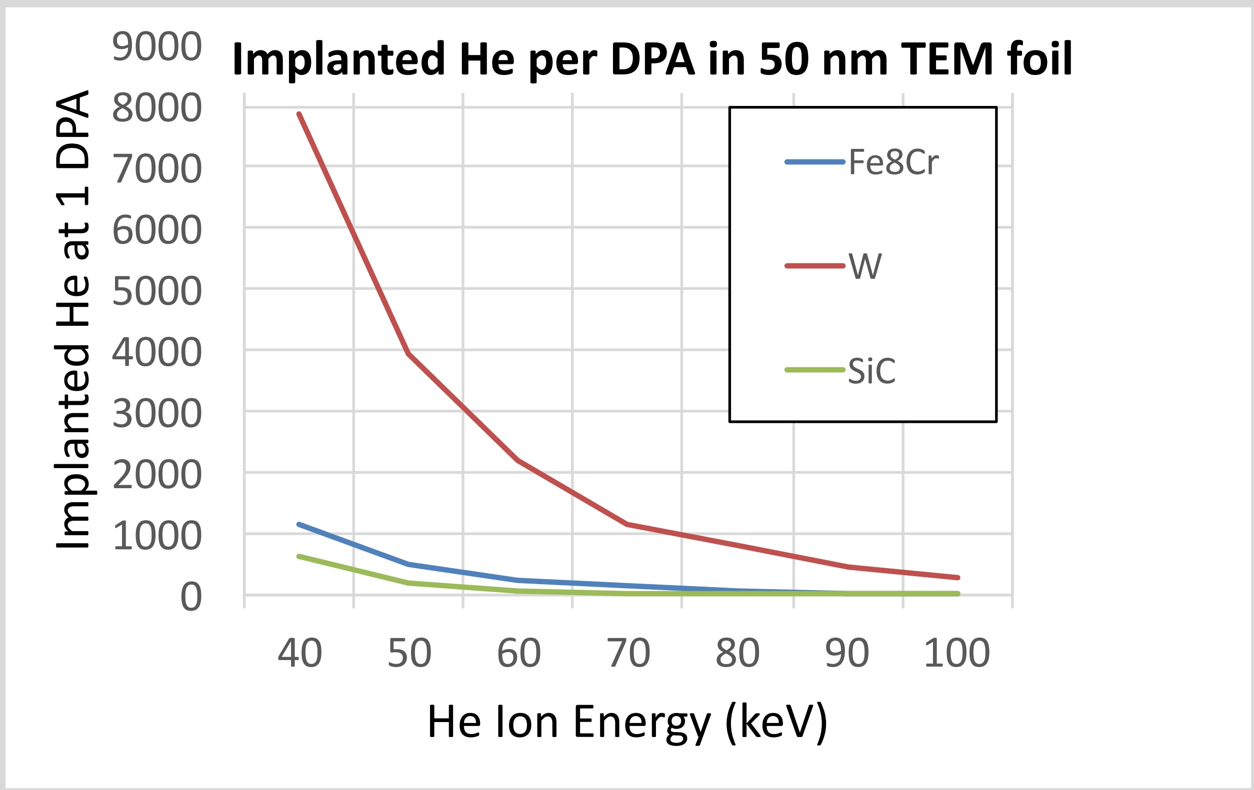

Alternatively, if two ion beams are available, displacement damage and He can be injected and controlled independently.

For thermal neutrons, incident on alloys containing significant amounts of nickel (e.g. austenitic steels), $R_{He/DPA}$ may be of order 100 appm/DPA whereas, for fast neutrons, a figure of 0.1 is likely. For fusion, $R_{He/DPA}$ is likely to be in the range 10–15 in structural alloys but will be higher (≈ 150) in SiC-based materials $R_{He/DPA}$ will thus vary by approximately 3 orders of magnitude across different types of reactor and different materials.

Nuclear Materials:
Tungsten

He irradiation of W: Effect of varying temperature and DPA

85 keV $He^{+} \rightarrow$ W

Explore damage morphology as a function of Temperature and DPA ($R_{He/DPA} \approx 500$)

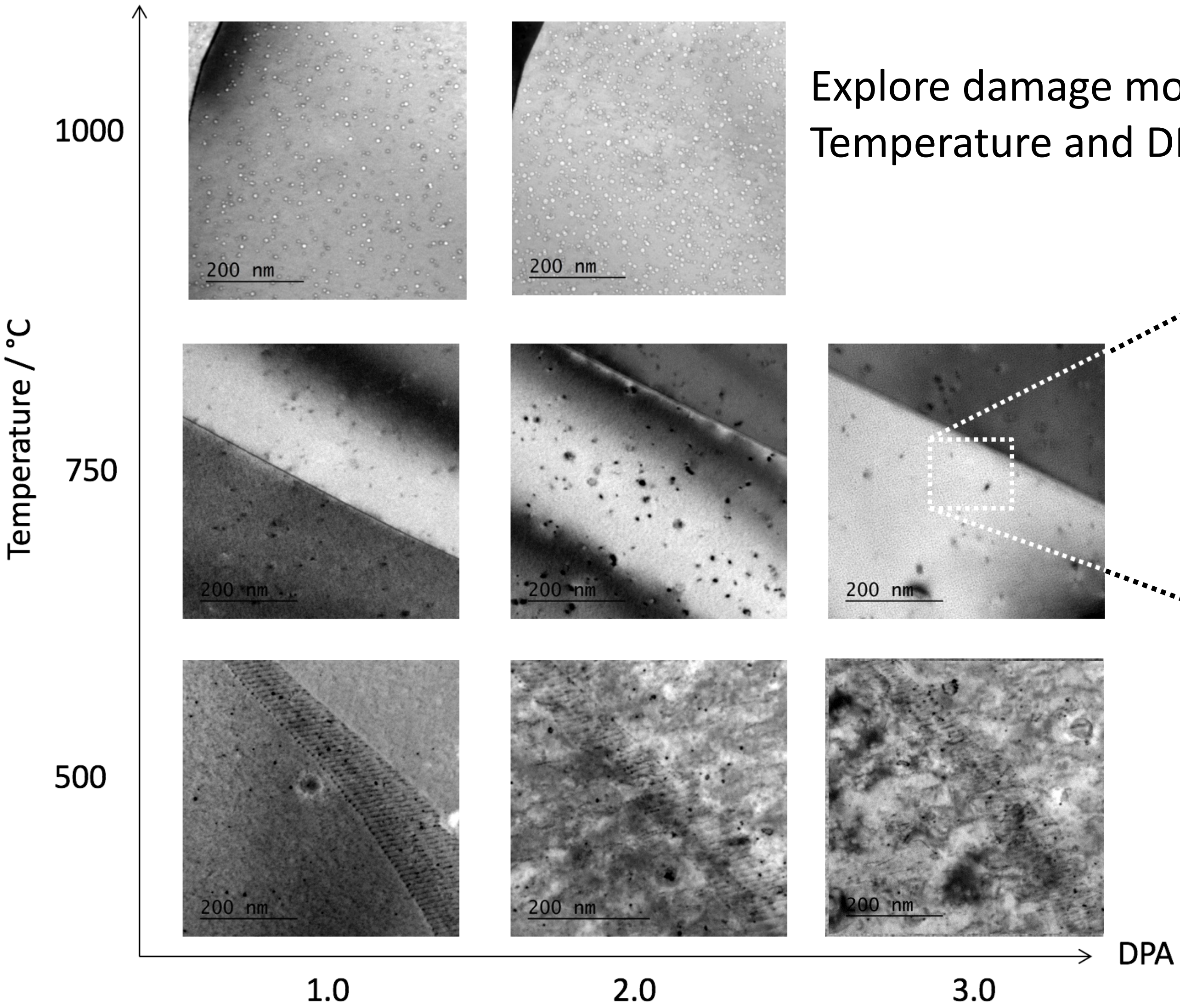

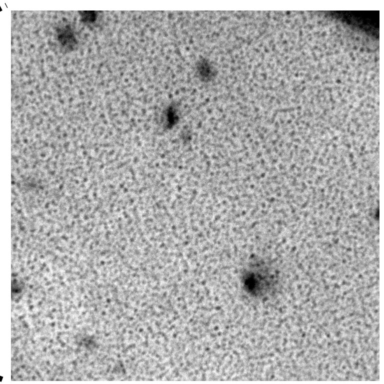

Alignment of bubbles.
Bubble superlattice

He Bubble Superlattices in W

W: 15 keV He$^+$, T = 500°C.   He appm/DPA ratio ~40,000

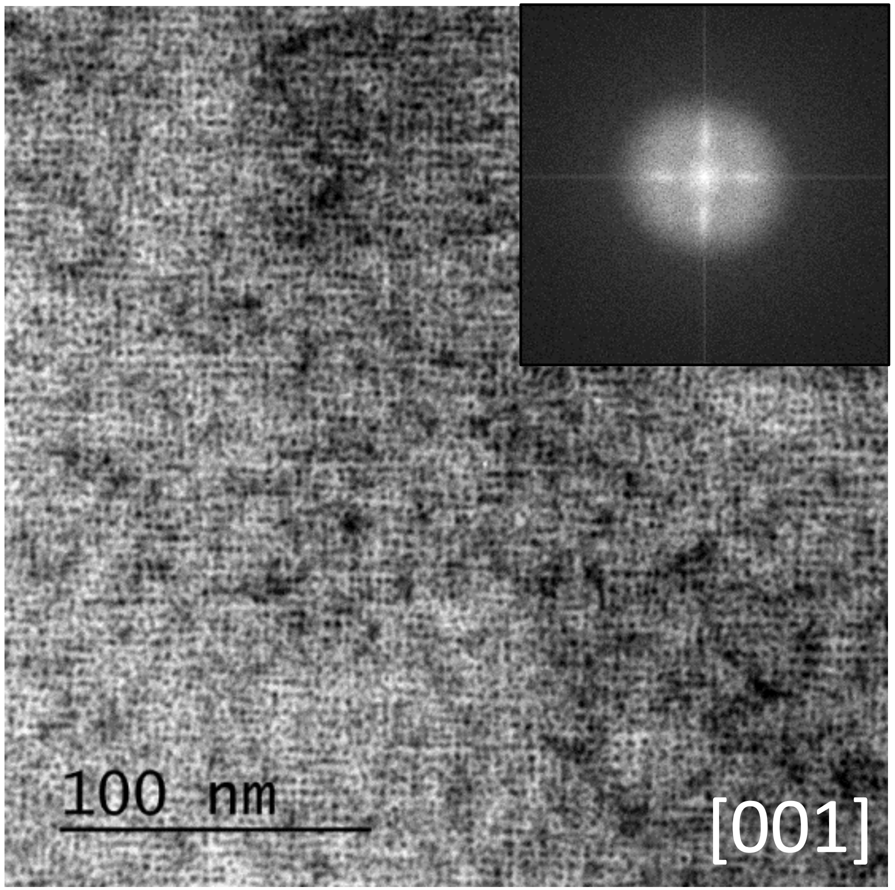

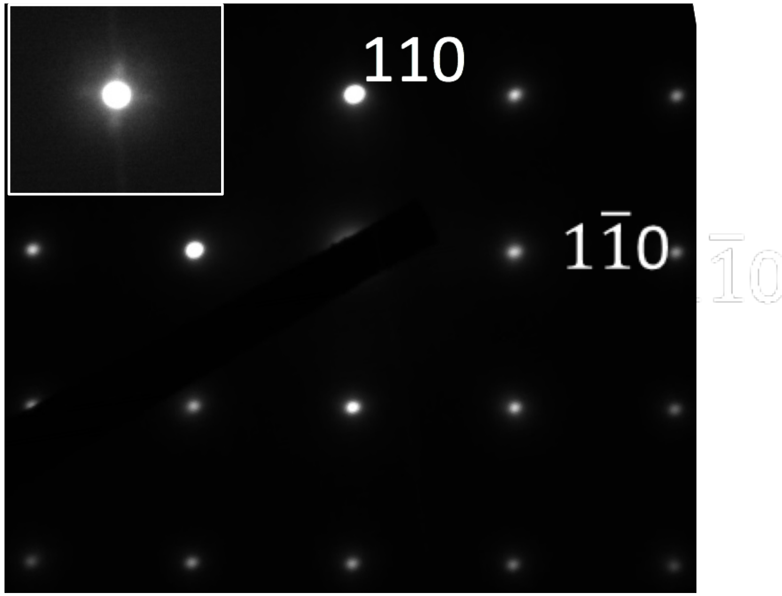

Lattice constant of helium bubble lattice,
a = 4.6 +/- 0.2 nm
Bubble density = 2.3 x 10^{19} He bubbles/cm^3

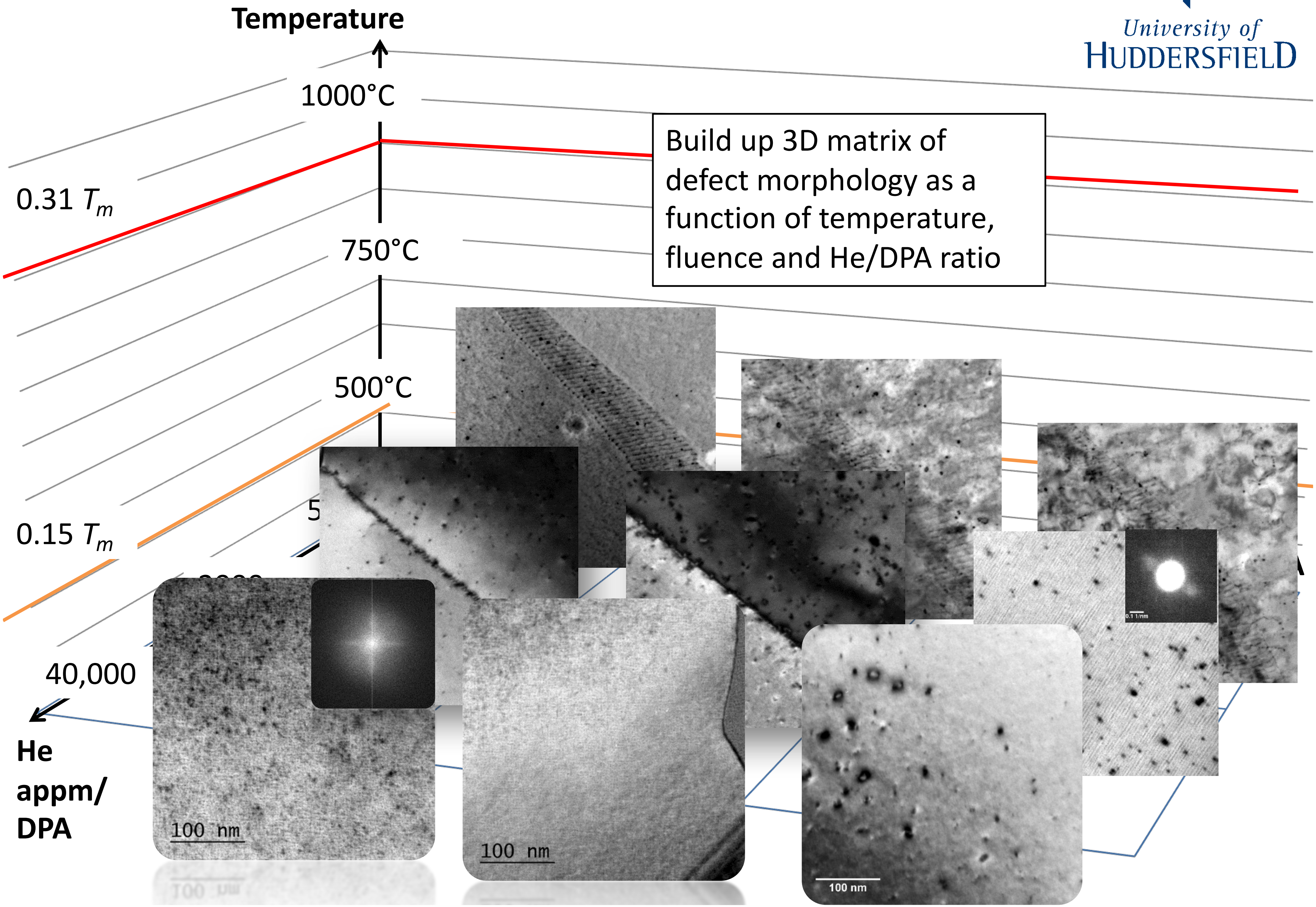

Build up 3D matrix of defect morphology as a function of temperature, fluence and He/DPA ratio

NUCLEAR MATERIALS:
Glasses

He/DPA Studies of Nuclear Glasses

In-situ experiments at MIAMI-1 in collaboration with Sylvain Peuget's group at CEA Marcoule. He/DPA ≈ 1.7% at%/DPA. 6 keV He at a flux of 10^{14} ions/cm^2/s. Temperature –130°C. SON68 glass.

Identification of threshold fluence for bubble nucleation correlates with free volume (SON68 N_s ~3×10^{21} sites.cm^{-3} ~2–3 at-%)

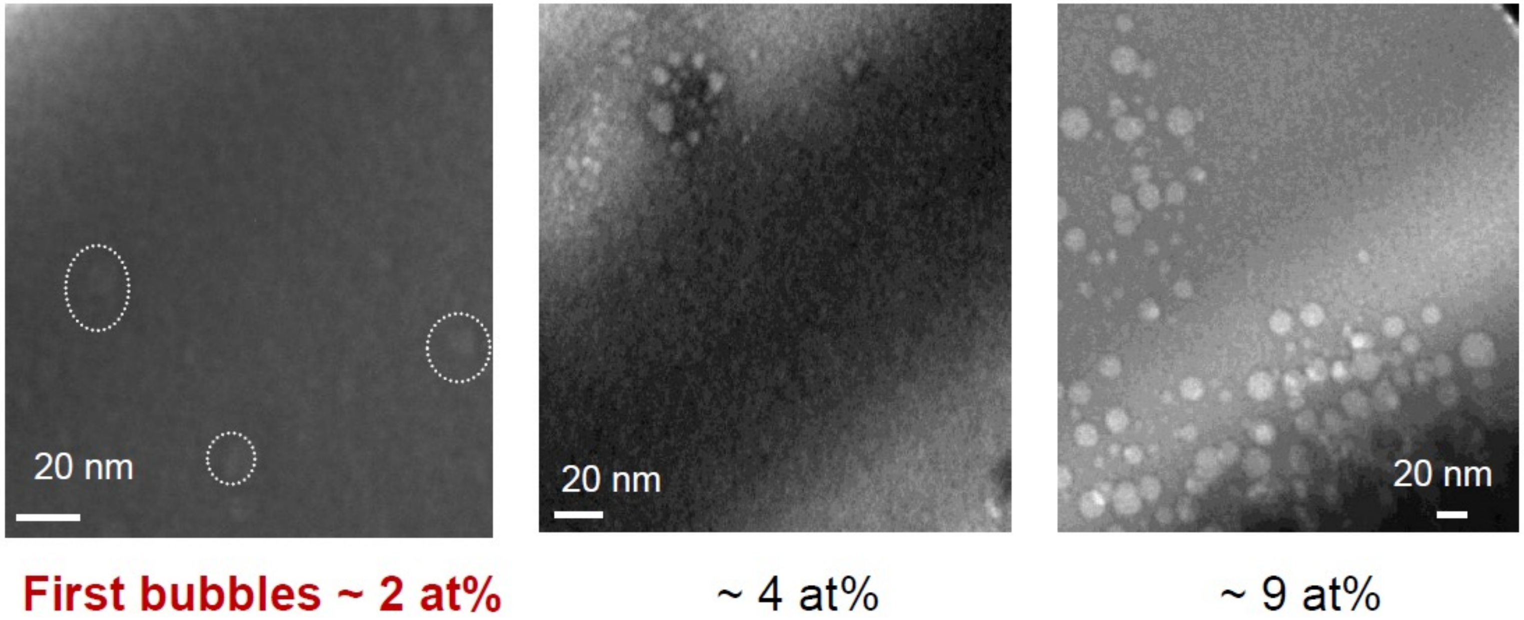

Non-uniform bubble distribution could be indicative of some inhomogeneities within the glass but areas with no bubbles are generally close to the edge of FIBbed lamellae.

Gutierrez et al, *JNM* **452** (2014) p565

He/DPA Studies of Nuclear Glasses

Continuation of irradiation to higher fluences:
He/DPA ≈ 1.7% at%/DPA. 6 keV He at a flux of 10^{14} ions/cm^2/s.
Temperature –130°C. SON68 glass.

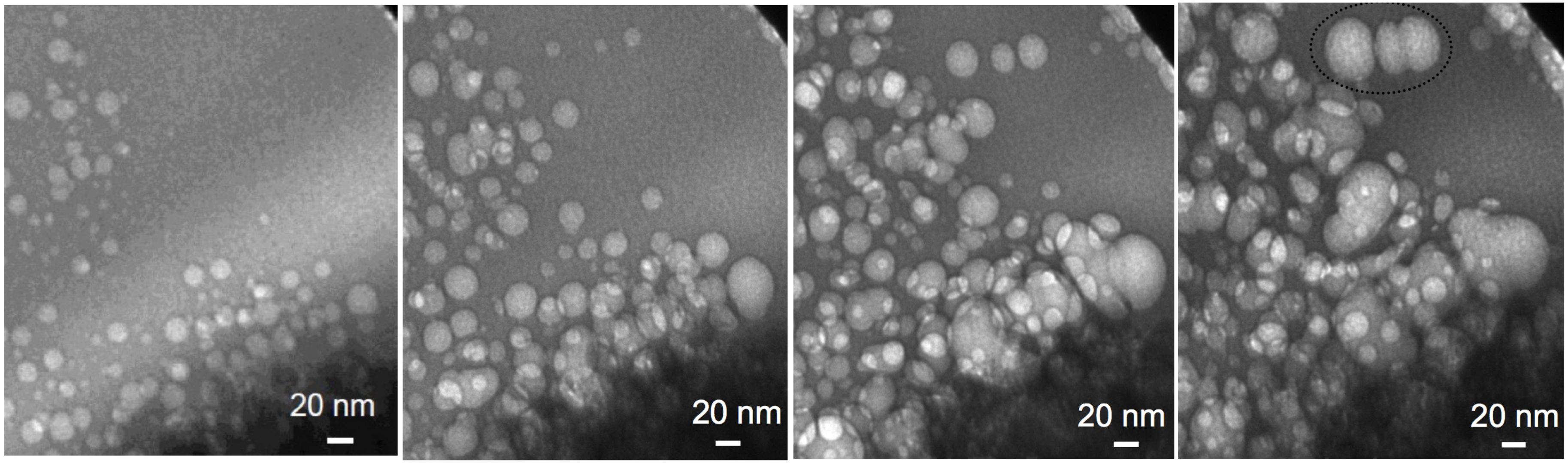

9 at% 14 at% 18 at% 23 at%

He/DPA Studies of Nuclear Glasses

University of Huddersfield

Similar experiments but with He/DPA ≈ 0.7 at%/DPA. 15 keV He at a flux of 10^{14} ions/cm^2/s. Temperature –130°C. SON68 glass

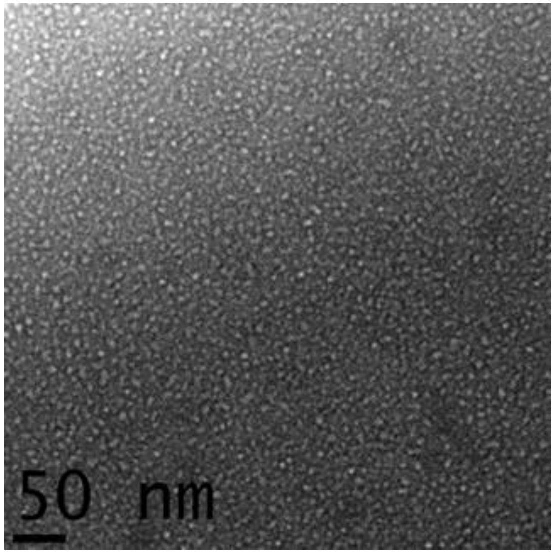

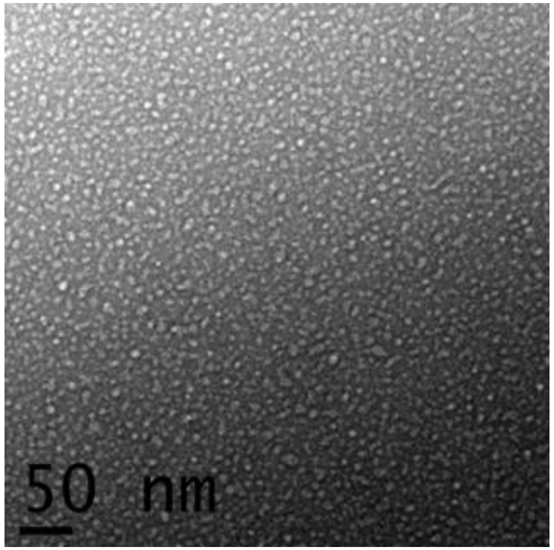

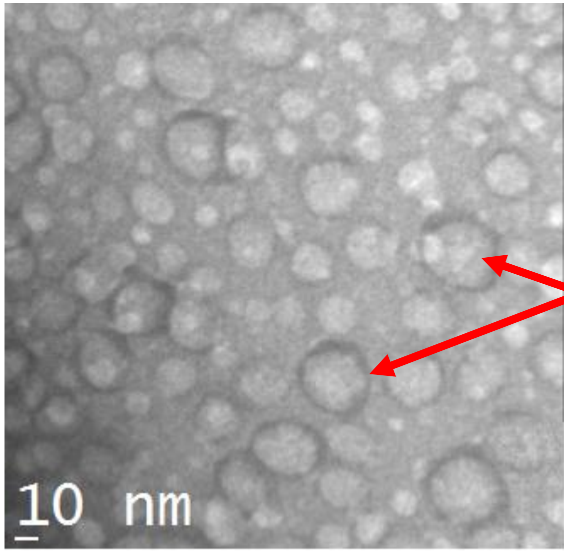

Blisters on surface

First bubbles ~ 0.2 at% | ~ 0.6 at% | ~ 9 at%

Additional damage (as a function of helium content) appears to result in a higher bubble nucleation density with nucleation occurring at a lower gas content. This needs to be verified by further experiments.

He/DPA Studies of Nuclear Glasses

University of HUDDERSFIELD

Effect of annealing on existing bubble population

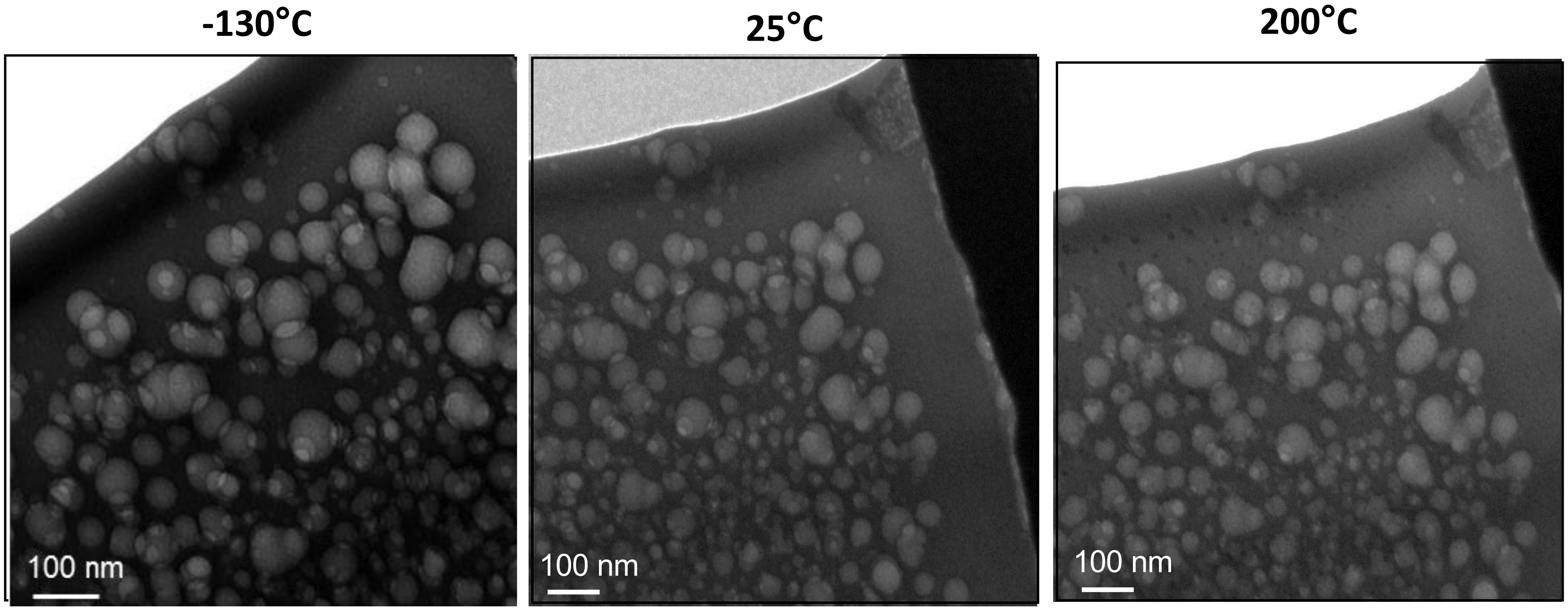

No change up to the glass transition temperature

Nuclear Materials:
Ceramics

6 keV He Irradiation of Perovskites

6 keV He irradiation of La $Fe_{0.8}$ $Al_{0.2}$ O_3 at room temperature. Flux ≈ 4.2×10^{13} He ions/cm^2/sec

Airy rings, indicative of formation of amorphous or nanocrystalline material are also seen at the high fluences (9×10^{16} He ions/cm^2).

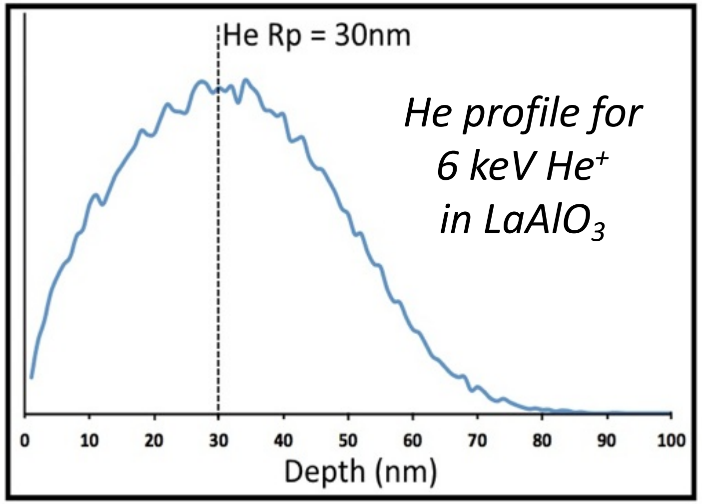

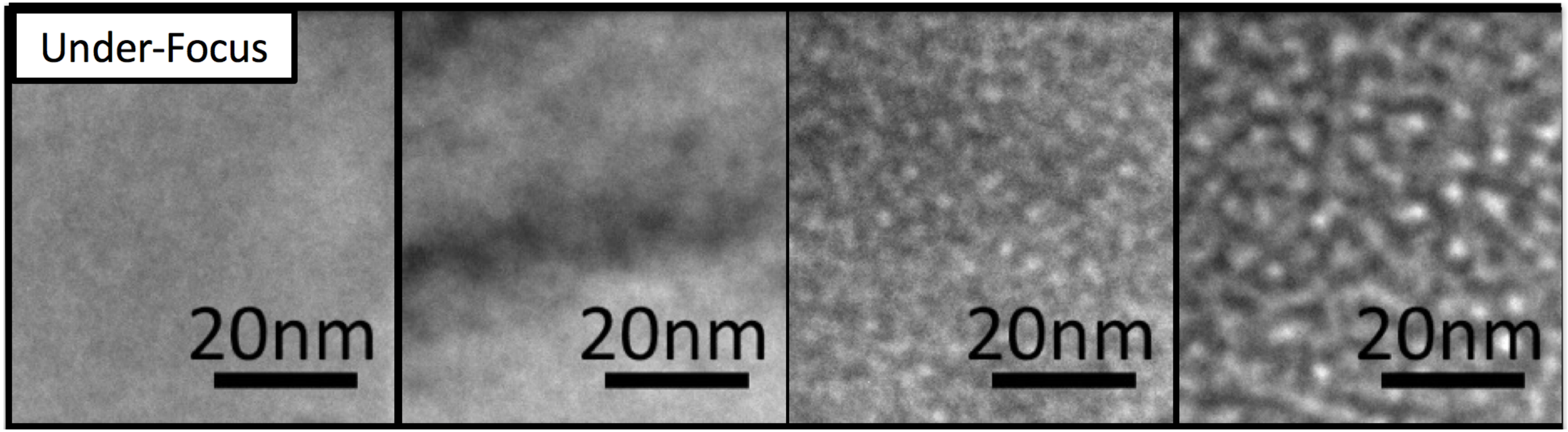

Before irradiation

4×10^{16} He ions/cm^2

5×10^{16} He ions/cm^2

9×10^{16} He ions/cm^2

Work by A. S. Gandy, University of Sheffield and K. Whittle University of Liverpool.

6 keV He Irradiation of Perovskites

Composition	Critical Fluence (He ions/cm^2)
$LaFeO_3$	-------
$LaFe_{0.8}Al_{0.2}O_3$	4.4×10^{16} He ions/cm^2
$LaFe_{0.6}Al_{0.4}O_3$	5.7×10^{16} He ions/cm^2
$LaFe_{0.4}Al_{0.6}O_3$	5.7×10^{16} He ions/cm^2
$LaFe_{0.2}Al_{0.8}O_3$	3.1×10^{16} He ions/cm^2
$LaAlO_3$	1.9×10^{16} He ions/cm^2

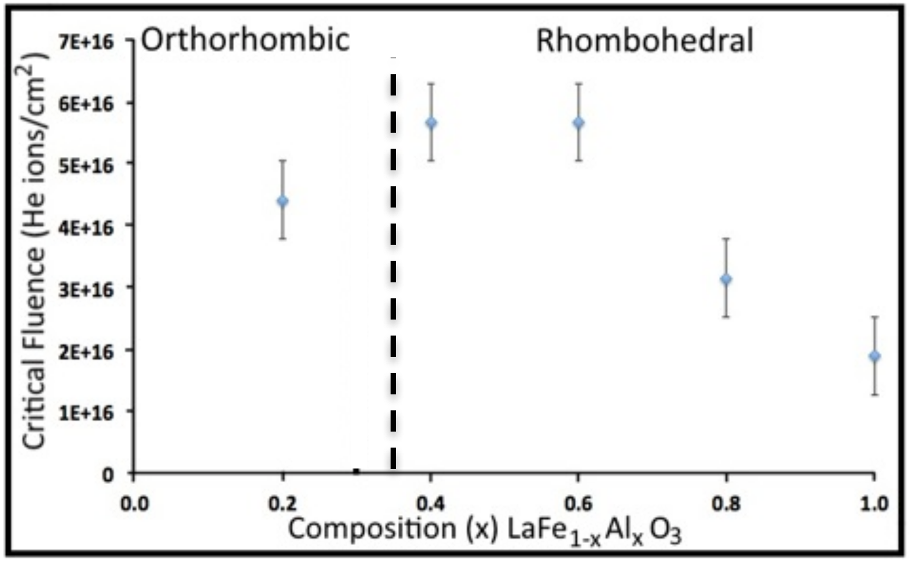

$LaFeO_3$ → $LaAlO_3$

- Critical fluence required for He bubble formation highest for $LaFe_{0.6}Al_{0.4}O_3$ and $LaFe_{0.4}Al_{0.6}O_3$, and lowest for $LaAlO_3$.

Work by A. S. Gandy, University of Sheffield and K. Whittle University of Liverpool.

University of HUDDERSFIELD

6 keV He Irradiation of Perovskites

$Ca_{0.6}\ La_{0.267}\ Ti\ O_3$

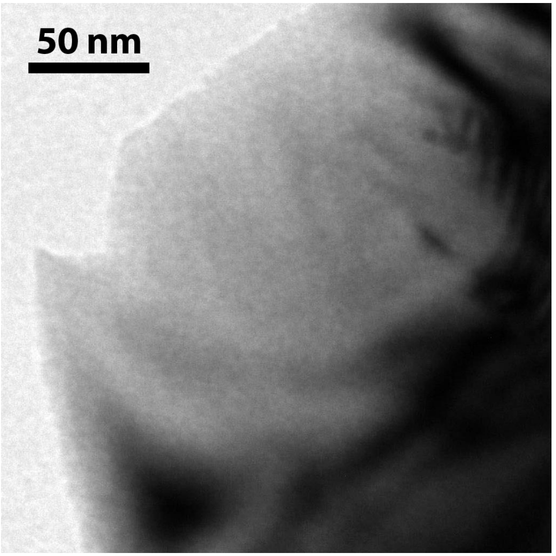

Unirradiated

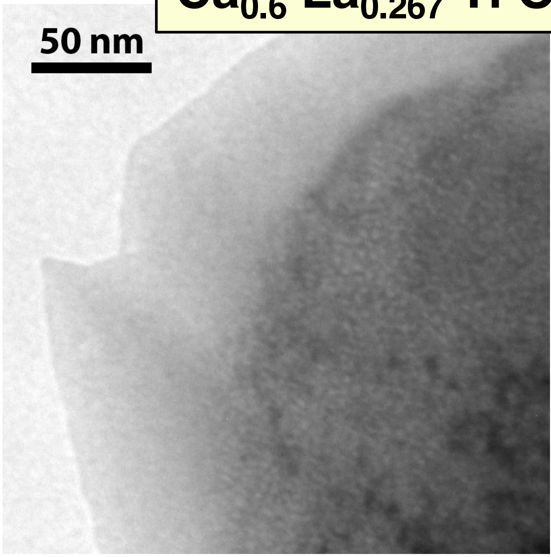

4.2×10^{16} ions/cm^2

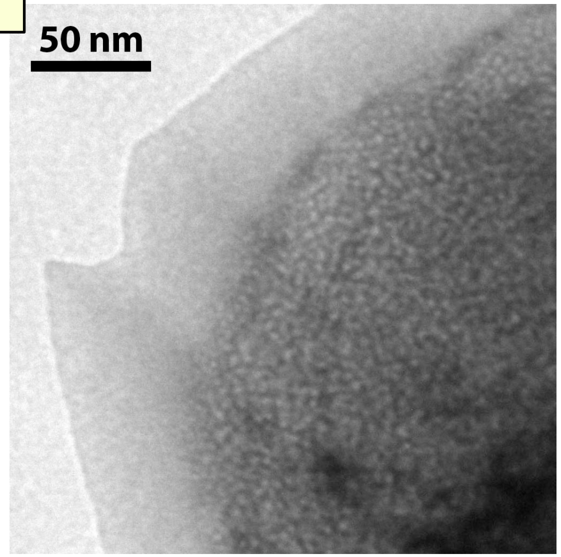

1.0×10^{17} ions/cm^2

In collaboration with S Lawson, A S Gandy & N C Hyatt, University of Sheffield

$Ca_{0.1}\ La_{0.6}\ Ti\ O_3$

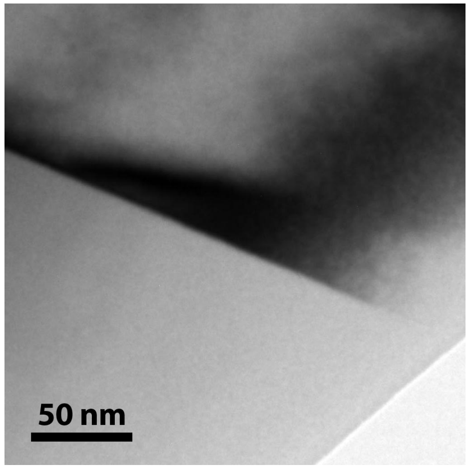

Unirradiated

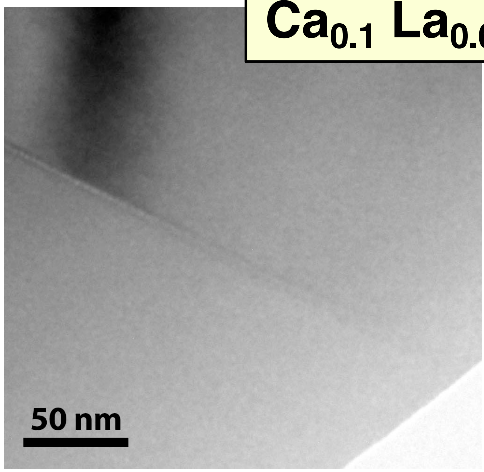

4.0×10^{16} ions/cm^2

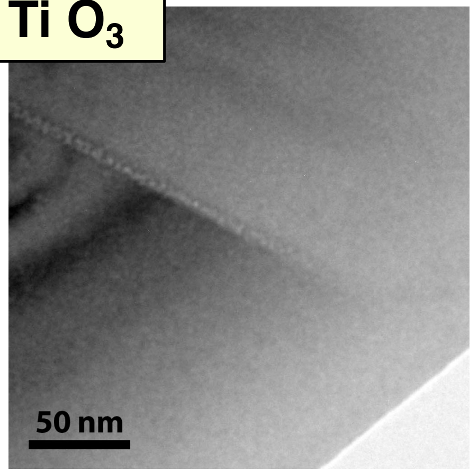

6.3×10^{16} ions/cm^2

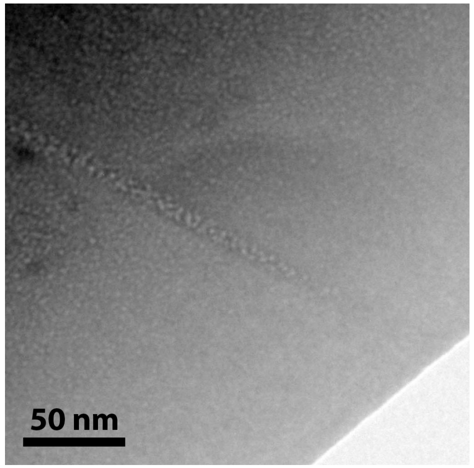

1.0×10^{17} ions/cm^2

He/DPA Studies of Nuclear Glasses

We are developing, a masking/heating holder to allow specific areas of a samples to be irradiated. This will be used to investigate the behaviour of helium in the ceramic, glass and at the interfaces in zirconolite glass-ceramic composites

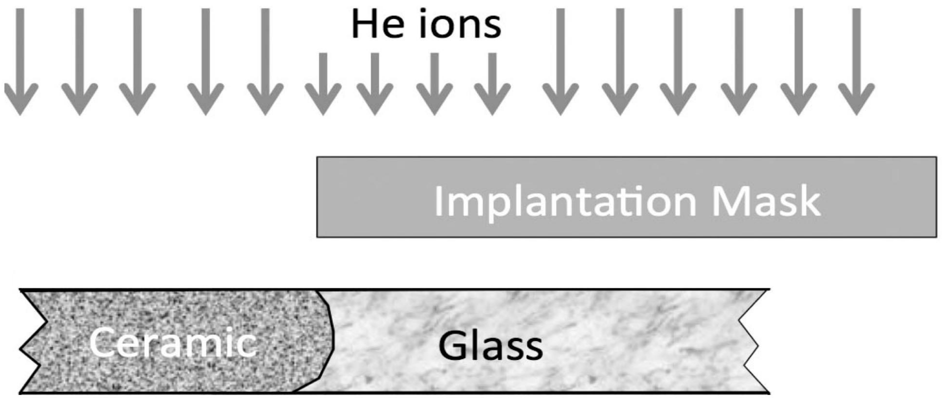

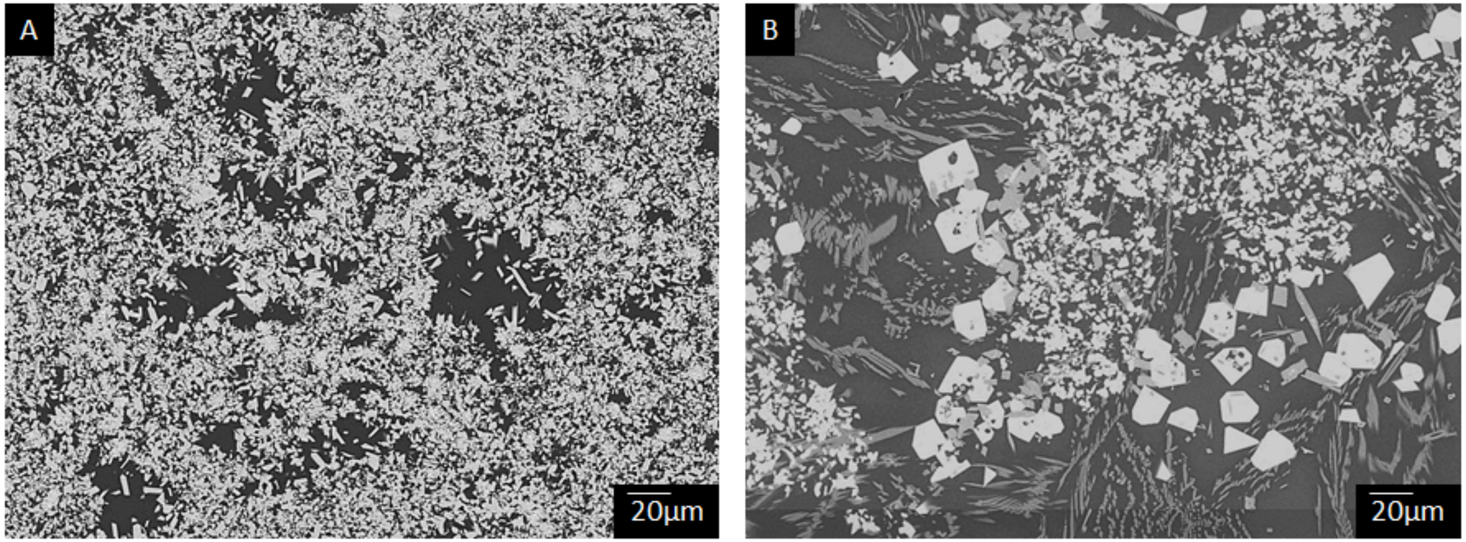

E. Maddrell, S. Thornber, N. C. Hyatt, J. Nucl. Mater. **456** (2015) 461-466.

Conclusions

I hope that I have convinced you that studies of ion-induced radiation damage in-situ in a transmission electron microscope can provide significant insights into a wide range of radiation-damage processes.

And also that experiments with ion beams can be used to simulate neutron damage –at least in order to explore qualitatively the fundamental processes involved. In this context, it is vitally important to collaborate with modellers in order to develop a atomistic-level understanding which may permit (cautious) quantitative extrapolation to neutron irradiation of bulk materials.

There are, however, a number of important caveats:

(i) It is always necessary to control for electron beam effects (comparison with areas of specimen not e-beam irradiated; beam-on, beam-off experiments, use of lower energy electrons . . .);

(ii) It is also necessary to compensate for accelerated timescale e.g. with temperature adjustments;

(iii) Close proximity of surfaces in TEM foils may greatly influence defect processes. Maybe, multiscale modelling can partially help in extrapolating to bulk materials.


Thank you
for
your attention

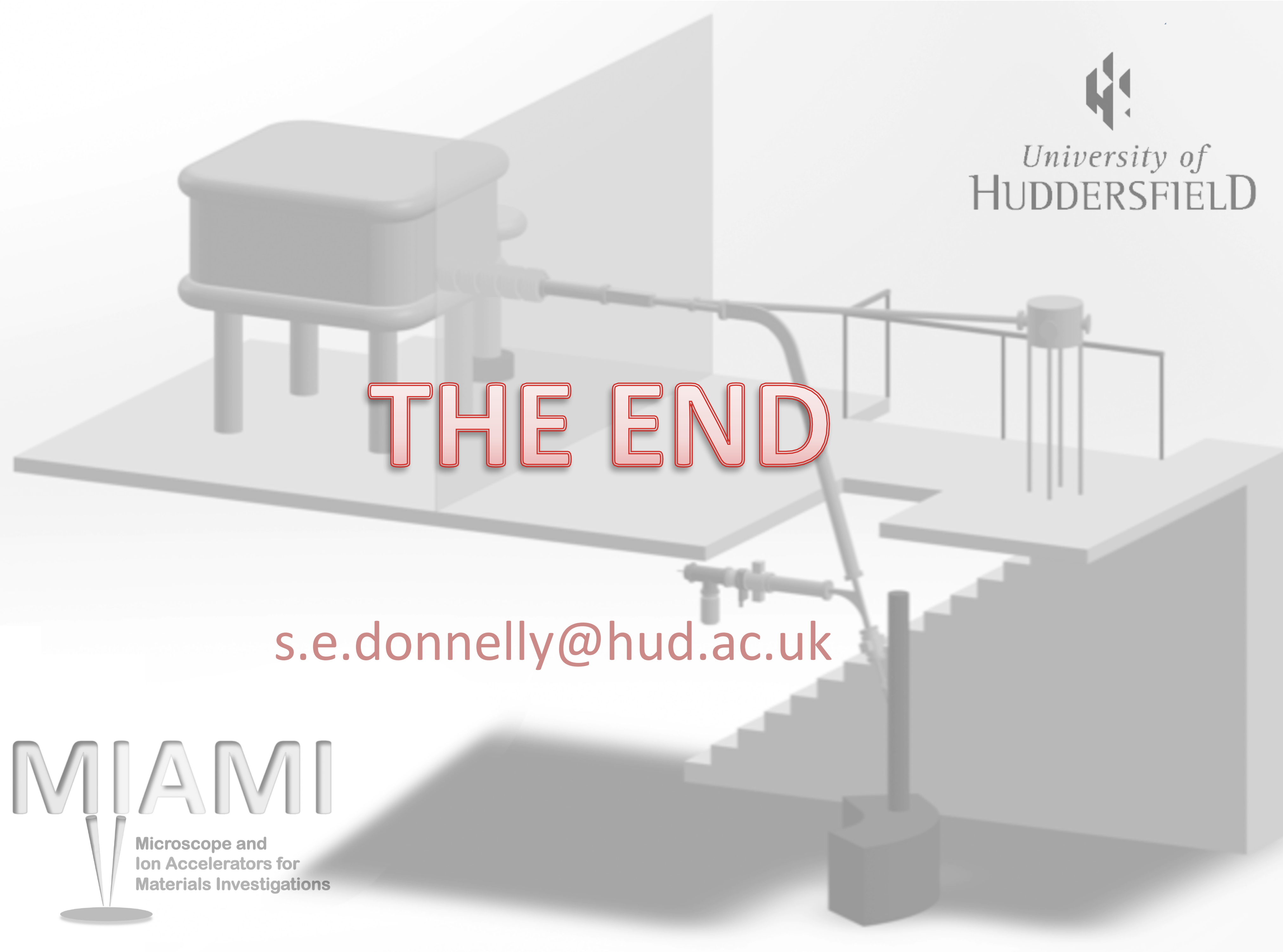

THE END

s.e.donnelly@hud.ac.uk

University of
HUDDERSFIELD

MIAMI
Microscope and
Ion Accelerators for
Materials Investigations